JPRS-JST-91-023
6 AUGUST 1991

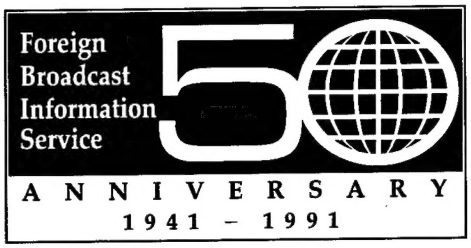

JPRS Report

Science & Technology

Japan

44TH MEETING ON CRYOGENICS AND SUPERCONDUCTIVITY

REPRODUCED BY
U.S. DEPARTMENT OF COMMERCE
NATIONAL TECHNICAL
INFORMATION SERVICE
SPRINGFIELD, VA 22161

JPRS-JST-91-023
6 AUGUST 1991

SCIENCE & TECHNOLOGY
JAPAN

44TH MEETING ON CRYOGENICS AND SUPERCONDUCTIVITY

916C0018 Tokyo TEION KOGAKU CHODENDO GAKKAI YOKOSHU in Japanese 23-25 Nov 90 pp 1-266

[Selected papers presented at the 44th Meeting on Cryogenics and Superconductivity held 23-25 Nov 90 at Yamagata University, sponsored by the Cryogenic Society of Japan]

CONTENTS

Preparation of Bi-Based Oxide Superconducting Fiber

916C0018 Tokyo TEION KOGAKU CHODENDO GAKKAI YOKOSHU in Japanese 23-25 Nov 90 p 1

[Article by Kazuhiko Hayashi, Hisao Nonoyama, and Masayuki Nagata, Osaka Research Laboratory, Sumitomo Electric Industries, Ltd.; and Kenichi Takahashi, Super-GM]

[Text] **1. Introduction**

We previously reported on the effect of growing speed on the structure and characteristics of Bi-Sr-Ca-Cu based oxide superconductors prepared by the laser pedestal process. To fabricate wires using superconductors in the future, it will also be necessary to achieve smaller growing size, capable of expecting flexibility, high-speed growth, and higher J_c. We mainly studied the effect of the growing size and speed on J_c, and report on the results obtained to date.

2. Experiment

Bi_2O_3, $SrCO_3$, $CaCO_3$, and CuO powders were mixed with each other in the composition ratio of $Bi_2Sr_2Ca_1Cu_2O_2$, and the mixture was temporarily sintered. Then, the temporarily sintered mixture was again sintered, and used as a starting raw rod. The growing size was changed by changing the diameter of the raw rod and the ratio of growing speed to feed rate of the raw rod. J_c of the specimen after annealing was measured by the four-probe method, with the growing size and speed being parameters. Then, the structure of the specimen's cross section was observed by optical microscopy and by SEM-EDX analysis.

3. Results

Figure 1 shows J_c (at 77.3 K, 0 T) of the specimen after annealing when the growing size and speed were changed. With a decrease in the growing size, high J_c was obtained, even if the growing speed was increased. Further I_c of practical level, i.e., 100 A or larger, was obtained where the growing size was 1.7 mmϕ. Structural observation revealed that a 2212 phase was oriented and formed along the orientation of the 0112 phase formed as grown by annealing. As the growing size becomes smaller, the 0112 phase is likely to be

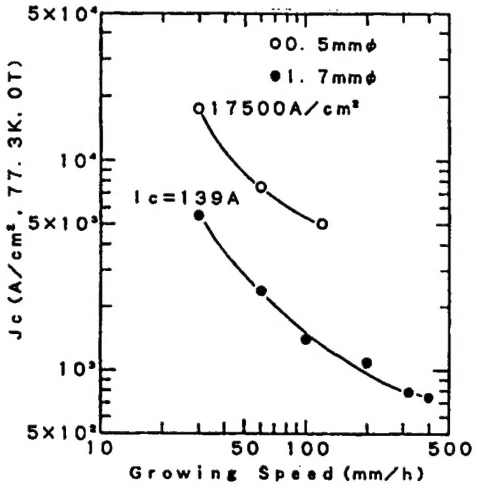

Figure 1. Relationship Between J_c and Growing Speed After Annealing

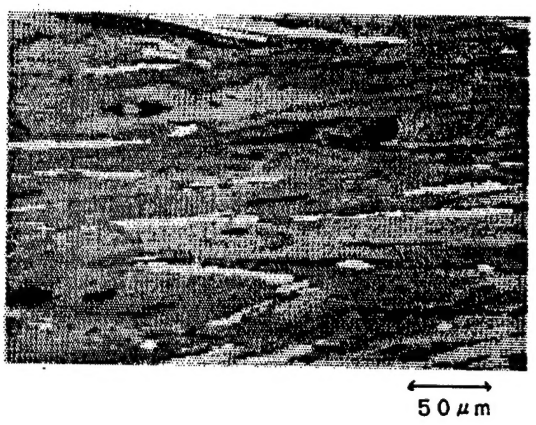

Photo 1. Structure of Longitudinal Section of Specimen After Annealing

oriented. In addition, the 2212 phase is satisfactorily oriented after annealing, and, therefore, J_c appears to become higher. Photo 1 shows the structure of a vertical section of the specimen that resulted in a J_c of 17,500 A/cm^2.

As a part of the Moonlight Project, "Superconducting Power Application Technology Development" established by the Agency of Industrial Science and Technology, MITI, this research was conducted under a contract from the New Energy/Industrial Technology Overall Development Organization (as a theme established by the Superconducting Power Generation-Related Equipment/Material Technology Research Association).

Preparation of Bi-Based Superconductors (1) (Horizontal Laser Heating Zone Melting Method)

916C0018 Tokyo TEION KOGAKU CHODENDO GAKKAI YOKOSHU in Japanese 23-25 Nov 90 p 2

[Article by Kazuhiko Tomomatsu, Atsushi Kume, and Nobuyuki Sadakata, Basic Research Laboratory, Fujikura, Ltd.; Masahiko Nakaide, Chikushi Hara, and Takahiko Yamamoto, Technology Research Laboratory, Tokyo Electric Power Co., Inc.]

[Text] **1. Introduction**

Bi-based superconductors are zonally melted and solidified on a tape base material, using horizontal laser zone-melting equipment. Thus, fine thick films whose crystals have an orientation are formed. In this way, we are conducting research on the preparation of wires using Bi-based superconductors. This time we studied the control of impurity phase formation and equalization of specimen thickness. In addition, we studied the relationship between thickness of specimen and crystal orientation, and between temperature distribution and crystal orientation, and report on these results below.

2. Preparation

Figure 1 shows an outline of the equipment used.

CO_2 laser beams, condensed to be long and narrow in the tape width direction, were irradiated on a superconductor powder applied on a tape base material, and a melt zone was formed. Then, by moving the tape, superconductor tapes were successively prepared. As a base material, an MgO (100) single crystal substrate was used, and raw powder with a $Bi_2Sr_2CaCu_2O_y$ composition was zonally melted at a speed of 10 mm/h. Changing the amount of raw powder, specimens ranging from 5~90 μm in thickness were prepared.

3. Results

Figure 2 shows the results of X-ray diffraction of as-grown powder of a specimen with a thickness of about 60 μm. The figure shows that a single phase specimen composed of 80 K phase was obtained as grown. It has been found that

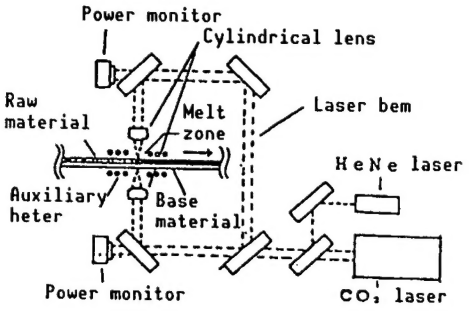

Figure 1. Schematic Drawing of Equipment

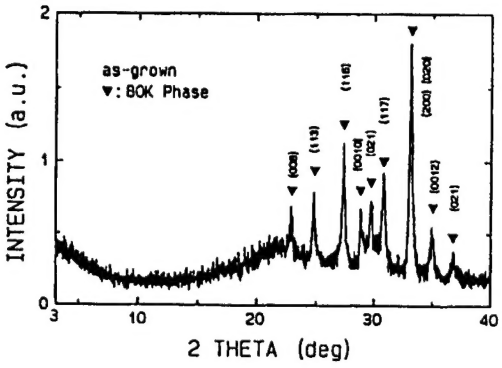

Figure 2. Results of Powder X-Ray Diffraction (as grown)

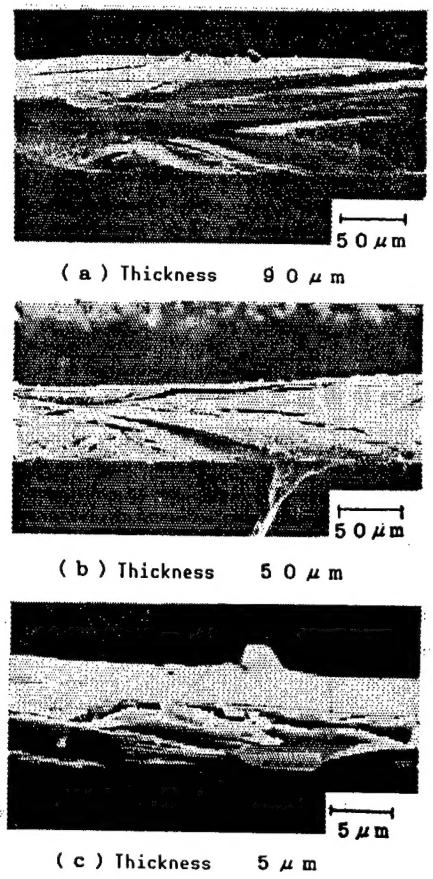

Figure 3. Results of SEM Observation on Longitudinal Section Fracture

the melting portion must be maintained at a uniform temperature to control the formation of impurity phases.

Figure 3 shows the results of SEM observation of a vertical section fracture of specimens with different thicknesses. These specimens are superconductors ranging from 5~90 μm in thickness. In each specimen, flat, layered crystals grew in the longitudinal direction, thus showing that each specimen has a superior crystal orientation. Specimens of 70 μm and 55 μm in thickness were heat treated at 840°C for 100 hours, and their I_c (J_c) were measured by the dc four-probe method (77 K, 0 T). As a result, 0.85 A (J_c = 550 A/cm) and 0.55 A (J_c = 740 A/cm) were obtained, respectively.

Preparation of Bi-Based Superconductors (2) (Horizontal Laser Heating Zone Melting Method)

916C0018 Tokyo TEION KOGAKU CHODENDO GAKKAI YOKOSHU in Japanese 23-25 Nov 90 p 3

[Article by Atsushi Kume, Kazuhiko Tomomatsu, and Nobuyuki Sadakata, Basic Research Laboratory, Fujikura, Ltd.; and Masahiko Nakaide, Chikushi Hara, and Takahiko Yamamoto, Technical Research Laboratory, Tokyo Electric Power Co., Inc.]

[Text] **1. Introduction**

As we have already reported, we paid attention to Ni as a substrate material for synthesizing superconductors, and melt solidified a temporarily-calcined Bi-based superconducting powder on an Ni substrate (on the surface of which an oxidized film was previously formed), using an electric furnace. Then, we heat treated the melt solidified powder in an appropriate manner, and prepared a superconductor. In this research, we formed a microscopic melt zone on an oxidized film formed on an Ni substrate, using laser beams, and provided solidified crystals with an orientation. Thus, we conducted research on the preparation of wires using Bi-based superconductors, while aiming at achieving higher J_c, and report on the method of preparation, results of observation of the crystal structure, superconducting characteristics, etc.

2. Experiment

An Ni substrate (2 mm width x 15 mm long x 0.2 mm thick) was heat treated, and an oxidized film (thickness: about 15 μm) was formed on the heat treated Ni substrate. Then, laser beams were condensed on a superconductor powder (composition Bi:Sr:Ca:Cu = 2:2:1:2) on the Ni substrate, and a melt zone was formed. An orientation for the crystal structure was provided during solidification, by moving the substrate. The specimen was further post heat treated at 820°C for 100 hours, and studied with regard to its superconducting characteristics.

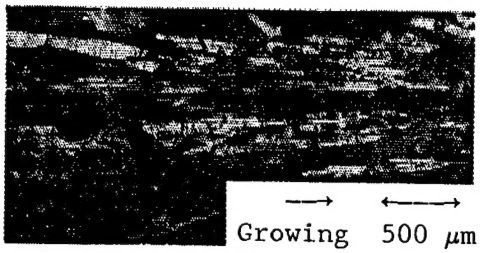

Figure 1. Specimen Surface Photographed by Optical Microscope (Substrate moving speed: 5 mm/h)

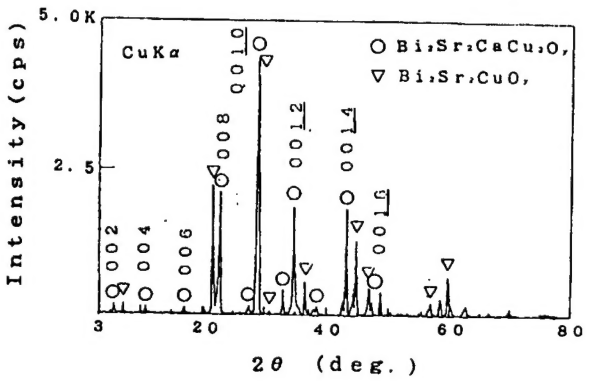

Figure 2. Results of X-Ray Diffraction of Specimen Surface Immediately After Melt Solidification

3. Results

Using the horizontal laser heating zone melting method, superconductor powder was melt solidified on the oxidized film formed on an Ni substrate (substrate moving speed: 5 mm/h). The specimen surface in this case was photographed by an optical microscope, as shown in Figure 1.

The figure shows that needle-shaped crystal grains have grown in the substrate moving direction. Figure 2 shows the results of X-ray diffraction of the surface of the specimen immediately after melt solidification.

The figure shows that a diffraction peak is strongly apparent on the $Bi_2Sr_2CaCu_2O_y$ (001) plane. It can be shown, therefore, that the 80 K phase is satisfactorily oriented. It has been found that the study of conditions to reduce formation of $Bi_2Sr_2CuO_y$ during melt solidification is one of the factors for improving superconducting characteristics.

Preparation of $10^4 A/cm^2$ Class Tl-Based Lengthy Wires

916C0018 Tokyo TEION KOGAKU CHODENDO GAKKAI YOKOSHU in Japanese 23-25 Nov 90 p 4

[Article by Tomoichi Hosono, Akira Nomoto, Tadashi Umezawa, and Masahiro Kiyofuji, Metal Research laboratory, Hitachi Cable, Ltd.; and Katsuzo Aihara, Hitachi Research Laboratory, Hitachi, Ltd.]

[Text] **1. Introduction**

Introduction of the pressing process makes it possible to provide oxide superconducting wires with highly superior characteristics. It is difficult, however, to fabricate lengthy wires by the general pressing process. Therefore, we studied the process of fabricating lengthy wires that have the characteristics equivalent to those of pressed wires. As a result, it has become possible to obtain lengthy wires with highly superior characteristics by developing a specific rolling process that shows deformation behaviors similar to those of the pressing process. We report below on the characteristics of tape-shaped wires fabricated by the specific rolling process and on the characteristics of pancake coils fabricated for trial using the tape-shaped wires.

2. Experiment and Results

(1) Fabrication of 10 m Wire

An Ag pipe was filled with 2223 phase Tl-based superconducting powder and was then drawn. The drawn Ag pipe was processed into a lengthy tape-shaped wire by the specific rolling process, and then heat treated to prepare a superconducting wire. Figure 1 shows the distribution of J_c of a wire (10 m in length) fabricated by this process. A 10 mm voltage terminal was provided at 1 m intervals to measure J_c of the wire. J_c of the wire was also measured over the entire length (10 m). Figure 1 shows that dispersion of J_c falls within ±2 percent and that $J_c = 10^4 A/cm^2$ has distributed uniformly. Even over the entire length of the wire, a voltage rapidly occurred at the critical current over zero resistance. It has been confirmed that the wire has a J_c of $10^4 Acm^2$.

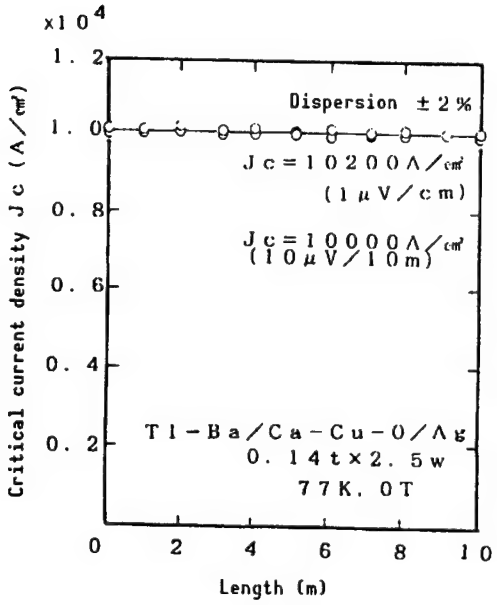

Figure 1. Distribution of J_c of Tape-Shaped Wire 10 m Long

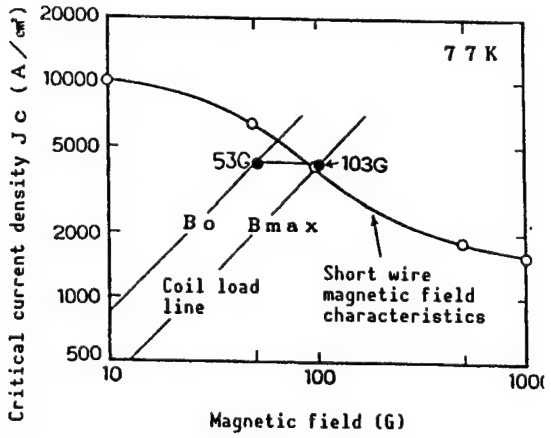

Figure 2. Characteristics of Pancake Coil

(2) Trial Manufacture of Coil

A pancake-shaped coil was fabricated using the Tl-based tape-shaped wire (10 m in length) and having the characteristics shown in Figure 1. The wind-and-react (W&R) process was employed for coil winding with consideration to bending distortion. For insulation, inorganic insulating materials were used to avoid adverse effects on the characteristics of the Tl-based tape shaped wire during heat treatment.[1] The coil fabricated is ϕ65 mm in outer diameter and ϕ30 mm in inner diameter.

The magnetic field characteristics of a short wire measured at 77 K and the coil load line are shown. With respect to coil characteristics, a central magnetic field of 53 G and a maximum magnetic field of 103 G were confirmed. The critical current value at the maximum magnetic field within the coil corresponded to the magnetic field characteristics of short wires. It can be shown, therefore, that the critical current as a coil is affected by deterioration of magnetic field generation, instead of by thermal stability.

References

1. Hosono, et al., '90 Spring Cryogenics Engineering Society Preliminary Draft C2-11.

Bi-Based Ag-Sheathed Wire Structure, J_c-B Characteristics

916C0018 Tokyo TEION KOGAKU CHODENDO GAKKAI YOKOSHU in Japanese 23-25 Nov 90 p 5

[Article by Mune Kamiyama, Takeshi Hyuga, Eiji Mukai, and Kenichi Sato, Osaka Research Laboratory, Sumitomo Electric Industries, Ltd.]

[Text] **1. Introduction**

It has already been made clear that the J_c–B characteristics of Bi–based high–temperature superconducting Ag sheathed wires are improved as the critical current density (J_c) is improved at 77.3 K, 0 T. We fabricated tape–shaped materials with various critical current densities, and studied their structures and J_c–B characteristics, and report on the results.

2. Experiment

Bi_2O_3, PbO, $SrCO_3$, $CaCO_3$, and CuO powders were mixed with each other so that a composition, Bi:Pb:Sr:Ca:Cu = 1.8:0.4:2.0:2.2:3.0, could be obtained. The mixture was temporarily sintered, put in an Ag pipe, underwent plasticity processing, and heat treated as a tape–shaped wire. Thus, a specimen was prepared. Then, the J_c–B characteristics of the specimen were measured at 4.2 K and 77.3 K. Along with this, the structure of the cross section of the specimen was observed.

3. Results and Discussion

Figure 1 shows the results of scanning electron microscope (SEM) observation of the cross section of a wire having enabled $J_c = 4.7 \times 10^4 A/cm^2$ to be obtained at 77.3 K, 0 T. With respect to the tape surface // B, the following critical current densities were obtained: $J_c = 3.1 \times 10^4 A/cm^2$ at 0.1 T; $J_c = 1.1 \times 10^4 A/cm^2$ at 1.0 T. The observation of the structure of the wire cross section revealed that nonsuperconducting phases, such as Ca_2CuO_3, are microscopically dispersed as J_c is improved at 77.3 K, 0 T.

Figure 2 shows J_c–B characteristics of various wires at 77.3 K. The figure shows that as J_c is improved at 77.3 K, 0 T, J_c–B characteristics are improved.

Figure 1. SEM Photograph of Ag/ BPSCCO Wire

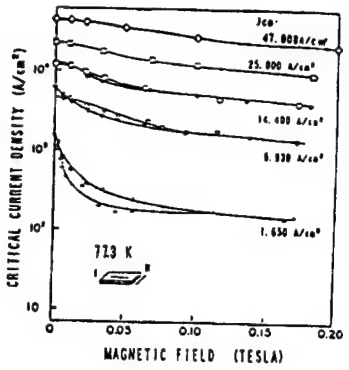

Figure 2. History Effects of Ag/BiPbSrCaCuO

Hysteresis existing in the specimens with a low current density has not been observed as the grain boundary weak bonding is improved, and J_c is thereby improved. Hysteresis is little observed in the specimens with J_c = 25,000 A/cm^2 or larger. A similar trend can be observed at 4.2 K.

We intend to report on J_c–B characteristics of the wires at 4.2 K, as well as the results of transmission electron microscope (TEM) observation at the meeting.

Preparation, Evaluation of Bi-Based Oxide Ag-Sheathed Tape

916C0018 Tokyo TEION KOGAKU CHODENDO GAKKAI YOKOSHU in Japanese 23-25 Nov 90 p 6

[Article by Katsuhiko Nomura and Masahiro Kiyofuji, Hitachi Cable, Ltd.; Kazumasa Togano, Hiroaki Kumakura, D.R. Diet Rich; and Hiroshi Maeda, National Research Institute for Metals]

[Text] **1. Introduction**

It has gradually been revealed that partial melting and annealing of Bi-based 2212 phase in the presence of Ag makes it possible to obtain a fine, well-oriented structure. Further, wires with such structure have so far attained high J_c values at 4.2 K in a high magnetic field. In the last report, we reported that of heat treatment conditions, a combination of partial melting temperature, cooling rate, and crystal growth temperature plays a vital role. In the vicinity of the Ag interface, a crystal orientation was observed in the direction along the interface. At the central part, there were nonoriented portions. Therefore, we further intend to study the fabrication conditions, while aiming at fabricating wires to which low temperatures and high magnetic fields are applied.

2. Experiment

We arranged in advance Bi-based 2212 phase powder, and processed this material into an Ag-sheathed tape by filling, drawing, and rolling processes in accordance with the procedures of the general Ag-sheathing process. Then, the processed Ag-sheathed tape was partially melted and annealed, and a Bi-based superconducting wire was thus fabricated. To study the heat treatment conditions, we conducted DTA-TG measurements, and studied prior heat-treatment for degasification. Further, we studied the thickness dependence of superconductor cores. With respect to superconducting characteristics, we measured critical current densities in a magnetic field of 4.2 K. In addition, we evaluated the results of microscopic structure observation by scanning electron microscope (SEM), optical microscope, etc.

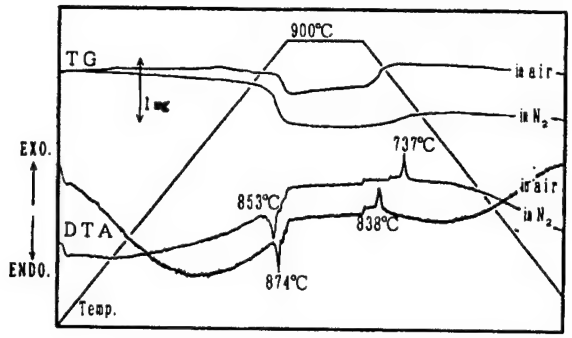

Figure 1. DTA-TG Measurement of Ag-Sheathed Tape

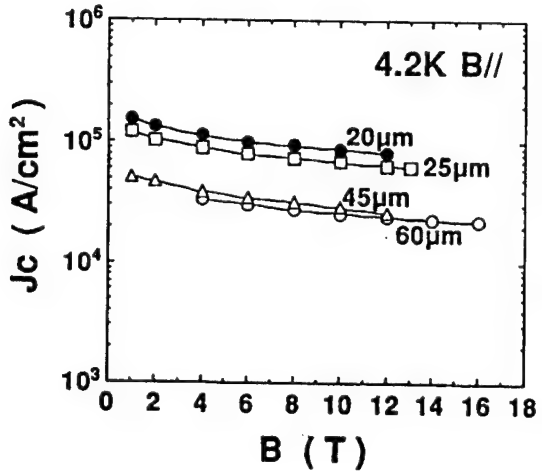

Figure 2. J_c-B Characteristics Based on SC Core Thickness

3. Results

The results of DTA-TG measurements (Figure 1) have revealed that oxygen enters and leaves the Ag-sheathed tape in a reversible manner during partial melting. Such behavior appears to blister the tape during the release of gas and thereby to interfere with crystal orientation. It has also been revealed that the melting point depends on oxygen partial pressures. Further, when the tape underwent prior heat treatment at 865°C, blistering decreased and J_c improved. Meanwhile, as the thickness of the superconducting core became smaller, J_c was improved. In other words, 10^6A/cm^2 (at 4.2 K, 6 T, B //) was achieved when the thickness of the core was 200 μm (Figure 2). SEM observation has also confirmed that an oriented structure has been formed over the entire area of the tape. To further improve the characteristics of the tape, we are studying the fabricating conditions.

External Magnetic Field Angle Dependence of Bi-Based Ag-Sheathed Tape

916C0018 Tokyo TEION KOGAKU CHODENDO GAKKAI YOKOSHU in Japanese 23–25 Nov 90 p 7

[Article by Kenji Shimohata, Shoichi Yokoyama, Toshie Takeuchi, and Shiro Nakamura, Central Research Laboratory; and Shoji Miyashita and Fumio Fujiwara, Material Research Laboratory, Mitsubishi Electric Corporation]

[Text] **Introduction**

The c-axis of oxide superconducting tape crystals is oriented vertically to the tape surface. An anisotropy, therefore, exists in both critical magnetic field and critical current density (J_c). These anisotropies, therefore, must be taken into account when preparing coils using oxide superconducting tape materials.

Experiment

Bi-based Ag-sheathed tape (thickness 0.2 mm, width 3 mm) with 2212 phase was melted at 890°C, annealed to 875°C, and calcined at this temperature for 60 hours. Thus, an oxide superconducting tape was obtained. J_c of this superconducting tape was measured by flowing current in the longitudinal direction on the tape surface, and changing the angle (θ) between the magnetic field and the tape surface (B $\perp$ I). The four-probe method was used for measuring. θ was determined by a hole device installed on the sample holder. The superconductivity rating criterion was a resistivity of $10^{-12}\Omega\cdot$cm.

Results and Discussion

Figure 1 shows the results of measurement of J_c (B, T, θ). A magnetic field was applied in parallel with and vertically to the tape surface, and J_c was measured in each case. At 4.2 K, the ratio (x) of J_c in the former case to that in the latter case was small, i.e., x = 1.6, irrespective of magnetic field. At 20 K, however, this ratio became larger, i.e., x = 3 when B = 1 T and x = 10 or larger when B = 5 T. At 30 K, this ratio amounted to x = 10 when B = 1 T.

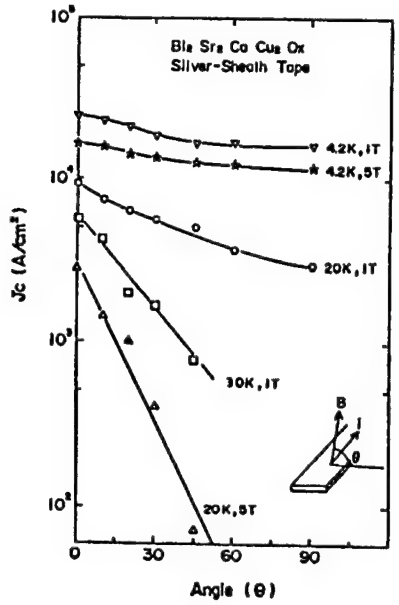

Figure 1. J_c (B, T, θ) Characteristics of Bi-Based Tape Material

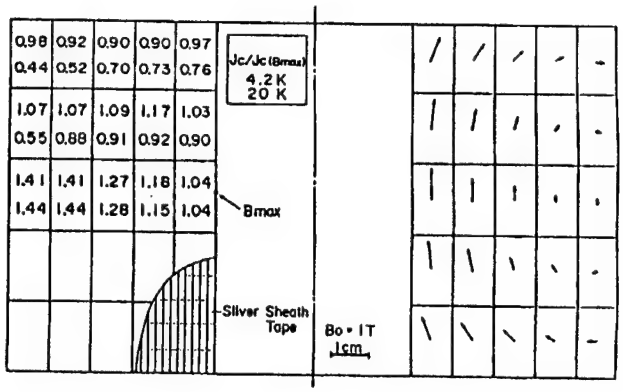

Figure 2. Magnetic Field Distribution and J_c of Each Point (Example of design of magnet using Bi-based tape materials)

Figure 2 shows an example of a coil design using Ag-sheathed tape materials (central magnetic field: 1 T, current density inside coil: 4,000 A/cm^2). Arrows show the intensity and direction of the magnetic field at each point. Further, J_c at each point, with J_c being established to be 1 at the B_{max} position, was indicated at the corresponding position. The point that determines the critical current of the coil is not on the inner circumference side but on the outer circumference side. The rate of lowering of J_c was small, i.e., 10 percent at 4.2 K, but amounted to 50 percent or more at 20 K.

Conclusion

When preparing coils using tape materials, it is necessary to pay attention to the magnetic field dependence of J_c. As the temperature rises, the effect of anisotropy becomes more and more conspicuous.

Characteristics of Bi-Based Superconducting Tape Wires

916C0018 Tokyo TEION KOGAKU CHODENDO GAKKAI YOKOSHU in Japanese 23-25 Nov 90 p 8

[Article by Sukeyuki Kikuchi, Naoki Uno, and Yasuzo Tanaka, Yokohama Research Laboratory, Furukawa Electric Co., Ltd.; and Chikushi Hara, Masahiko Nakaide, and Takahiko Yamamoto; Technology Research Laboratory, Tokyo Electric Power Co., Inc.]

[Text] **1. Introduction**

Various experiments and studies of the Ag-sheathed tape wire fabricating process have been conducted. A superior J_c of order of $10^4(A/cm^2)$ has already been reported for Bi-based superconducting tape wire specimens of several centimeters in length. To put such wires into practical application, however, it is necessary to fabricate longer ones. We conducted experiments on changes in the characteristics where the length of the tape wires (prepared by the conventional method) was increased, and report on the results.

2. Experiment

Powders of Bi_2O_3, $SrCO_3$, $CaCO_3$, and CuO were blended and mixed so that the required composition could be obtained. The resultant mixture was temporarily calcined in air at 800°C for 50 hours, and was then pulverized. This temporarily calcined powder was molded by cold isostatic pressing (CIP) into a round bar. The round bar was inserted in an Ag pipe which, in turn, was vacuum sealed to prepare a billet. The billet underwent swaging, rolling, etc. Thus, tape wires with various thicknesses and widths were fabricated. These tape wires were cut into different lengths and were heat treated; their characteristics were measured.

The critical current density J_c was measured by the dc four-probe method. Further, a distribution of J_c in the longitudinal direction of each tape was measured. J_c was also measured for the case where the distance between voltage terminals was increased. Magnetization of some specimens was also measured.

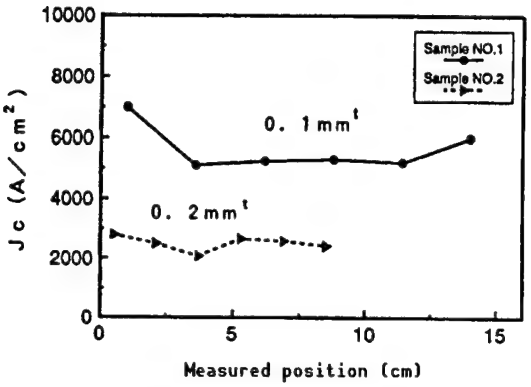

Figure 1. Distribution of J_c of $Bi_2Sr_2CaCu_2O_x$ System Ag-Sheathed Tape Wire in Longitudinal Direction

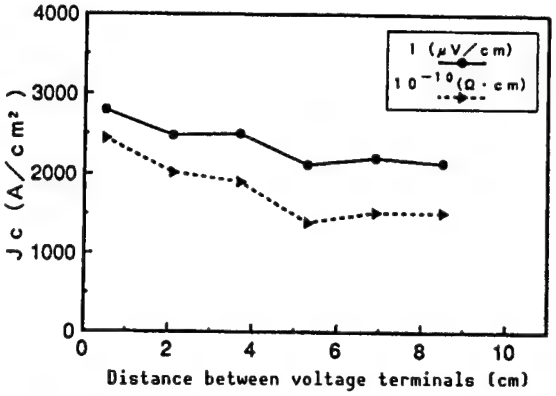

Figure 2. Relationship Between Inter-Voltage Terminal Distance and J_c (Tape thickness: 0.2 mm)

3. Results

(1) Figure 1 shows a distribution of J_c of typical $Bi_2Sr_2CaCu_2O_x$ system Ag-sheathed tape wires (thickness: 0.1 and 0.2 mm, length: about 10 and 15 cm) in the longitudinal direction. The distance between the voltage terminals was 10 mm. The criterion was constant, i.e., 1 μV/cm. The figure shows that there is no large change in J_c on the whole, but that there are some parts whose J_c was partially lowered. Magnetization of the portions whose J_c was different from each other was measured. As a result, it was shown that there is no difference in magnetization between the two types of tapes. It is thought, therefore, that the partial lowering of J_c is attributable to the linkage of superconductors.

(2) Figure 2 shows changes in J_c where the distance between the voltage terminals was increased from one end with respect to sample 2 (thickness: 0.2 mm, length: about 10 cm). The criteria were 1 (μV/cm) and $10^{-10}(\Omega\cdot cm)$.

The presence of partially low J_c portions affect the entire J_c. It has been found, therefore, that it is necessary to fabricate tape wires whose J_c does not change greatly in the longitudinal direction.

We intend to report on the characteristics of longer tape wires at the meeting.

Conclusion

When preparing coils using tape materials, it is necessary to pay attention to the magnetic field dependence of J_c. As the temperature rises, the effect of the anisotropy becomes more and more conspicuous.

Superconducting Characteristics of Bi-Based Ag-Sheathed Tape

916C0018 Tokyo TEION KOGAKU CHODENDO GAKKAI YOKOSHU in Japanese 23-25 Nov 90 p 9

[Article by Kazuo Yamamoto and Akatsuki Murase, General Research Laboratory, Toshiba Corporation; and Hiroshi Kitamura and Takayao Hasegawa, Showa Electric Wire & Cable Co., Ltd.]

[Text] **1. Introduction**

It has already been reported that the reduction of oxygen partial pressure in a heat treatment atmosphere proves to be effective for changing Bi-based high T_c phase bulks into single phases.[1] It is thought that the reduction of oxygen partial pressures makes it possible to facilitate the formation of high T_c phases in the core, even in the case of Ag-sheathed tapes. In this research, the oxygen partial pressure in the atmosphere was reduced to 7.7 percent, and then tape specimens were heat treated. Thus, their microscopic structure and superconducting characteristics were studied.

2. Experiment

The tape specimen preparation conditions before rolling were the same as those publicized at the previous meeting.[2] For this experiment, tapes at 0.15 mm and 0.1 mm in thickness were prepared and heat treated at 835°C for 50 hours. Further, they were intermediately pressed and heat treated (in a 7.7 percent O_2 + Ar atmosphere) twice. The critical current I_c of specimens was measured by the four-probe method. Their crystal structures were analyzed and observed by X-ray diffraction and scanning electron microscope (SEM).

3. Results

Figure 1 shows the intermediate press pressure dependence of J_c (77 K, 0 T) with respect to the tapes heat treated in a 7.7 percent O_2 + Ar atmosphere. For the 0.1-mm thick tapes, the J_c of the tape pressed twice was compared with that of the tape pressed once. As a result, it has been found that only the absolute value of J_c was improved, although the shape of the press pressure dependence curve was little changed. In other words, J_c increased nearly in proportion to the press pressures, up to a press pressure of 15 t/cm^2.

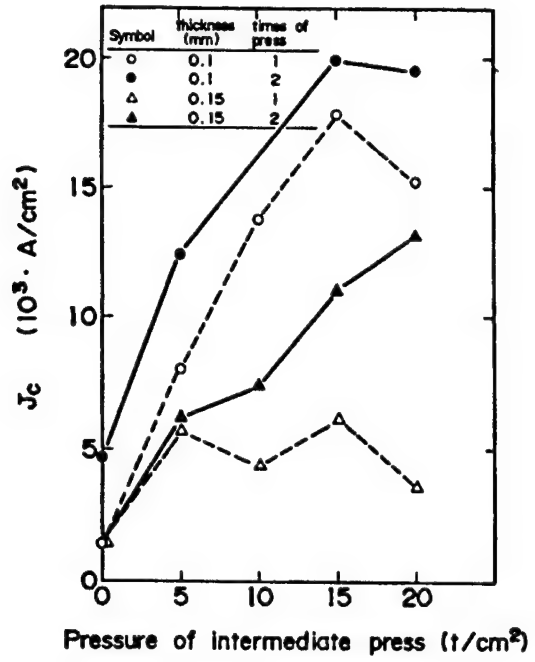

Figure 1. Press Pressure Dependence of J_c (77 K, 0 T)

J_c showed a tendency to saturate at press pressures from 15 t/cm2 to 20 t/cm2. A maximum J_c of 20,000 A/cm^2 was obtained for the tape pressed twice.

Meanwhile, for tapes that were each 0.15 mm thick, a large change was observed in the press pressure dependence of J_c between the tape pressed once and that pressed twice. The J_c of the tape pressed once did not depend on press pressures at 5 t/cm^2 or larger, and showed approximately constant values. The J_c of the tape pressed twice, however, increased in proportion to press pressures, up to 20 t/cm^2.

At the meeting, we will report on the cause of changes in the press pressure dependence of J_c due to different tape thickness, and the difference in heat treatment between the 7.7 percent O_2 + Ar atmosphere and the atmosphere, based on the results of X-ray diffraction and SEM observation.

References

1. Koyama, S., et al., JPN. J. APPL. PHYS., Vol 27, 1988, p L1861.

2. Yamamoto, et al., Cryogenics Engineering/Superconductivity Society, preliminary draft for 1990 spring meeting, p 218.

Ag-Sheathed $Bi_2Sr_2CaCu_2O_y$-Based Superconducting Tape

916C0018 Tokyo TEION KOGAKU CHODENDO GAKKAI YOKOSHU in Japanese 23-25 Nov 90 p 10

[Article by Junichi Kai, Keisuke Yamamoto, and Makoto Hiraoka, Central Research Laboratory, Mitsubishi Cable Industries Co., Ltd.]

[Text] **1. Introduction**

It has already been reported that oriented structures in Bi-based 2212 phase can be obtained by growing crystals from the partially melted state and that higher J_c can be obtained.[1] This process was applied to Ag-sheathed tapes. As a result, where the tape was heat treated at temperatures near the partial melting temperature, the growth of coarse Sr-Ca-Cu-O system nonsuperconducting crystal grains was markedly observed. These coarse crystal grains are likely to prevent the targeted orientation of crystals and to cut the flow of superconducting transportation current. Therefore, we attempted to control the formation of nonsuperconducting phases by adjusting the mix composition of Bi-based oxide superconducting calcined powders that are used as raw materials.

2. Experiment

Starting raw materials, i.e., Bi_2O_3, $SrCO_3$, $CaCO_3$, and CuO powders were mixed in the ratios given in Table 1, calcined at 820°C for 12 hours, and pulverized three times; thus, calcined powders were obtained. The calcined powders were molded by cold isostatic pressing (CIP), cut in the form of pellets which, in turn, were heat treated at 870°C for 60 hours. Thus, specimens were obtained. The crystal phase of the specimens obtained was identified by SEM (EDX), and the ac susceptibility characteristics were also evaluated.

Table 1. Mix Composition Ratio (Unit: Atomic ratio)

	Bi	Sr	Ca	Cu
I	2.0	2.0	1.0	2.0
II	2.0	2.0	1.17	2.17
III	2.0	2.0	0.64	1.64

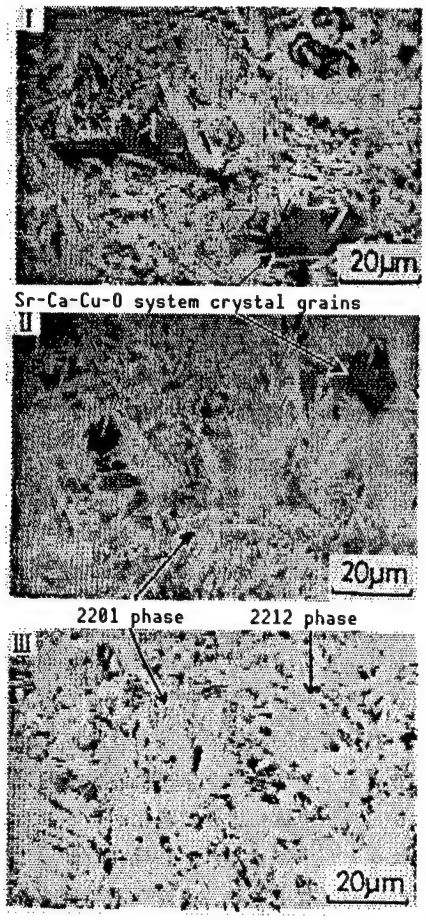

Figure 1. SEM (BEI) Image of Each Specimen

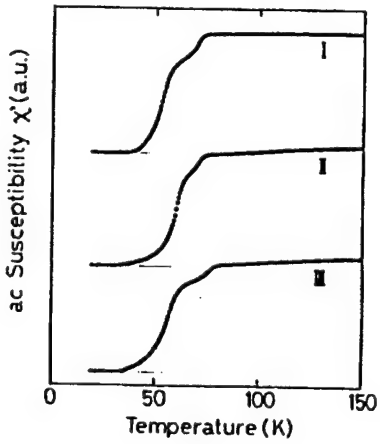

Figure 2. Temperature Dependence of ac Susceptibility (θ') of Each Specimen

3. Results

Figure 1 shows a SEM (BEI) image of each specimen. The 2201 phase can be slightly observed in the composition III specimen, although no Sr-Ca-Cu-O system crystal grains as observed in other specimens can be seen.

Figure 2 shows the temperature dependence of ac susceptibility (θ') of each specimen. Although each specimen showed phase transition in two stages, no large difference could be observed in the temperature dependence of 2212 phase θ'. From this, it can be thought that in composition III, the growth of Sr-Ca-Cu-O system crystal grains was almost completely controlled by adjusting the composition without impairing the characteristics of 2212 phase. We intend to report on the results of application of this process to Ag-sheathed wires at the meeting.

References

1. Kumakura, H., CRYOGENICS ENGINEERING, Vol 25 No 2, 1990, p 88.

Fabrication of High I_c Oxide Superconducting Composite Wires Using Doctor Blade Process

916C0018 Tokyo TEION KOGAKU CHODENDO GAKKAI YOKOSHU in Japanese 23-25 Nov 90 p 11

[Article by Noritsugu Enomoto and Naoki Uno, Furukawa Electric Co., Ltd.; and Kunio Doi, Super-GM]

[Text] **Introduction**

To apply oxide superconductors to electric power, it is necessary to compound high critical current (I_c) and stabilizing metals. The conventional wire fabrication processes have so far made it possible to obtain high critical current density (J_c), but have made it difficult to achieve high I_c. We fabricated multilayered wires by compounding uniformly layered compacts (tens to hundreds μm)—obtained by the doctor blade process—and Ag sheets in the specified ratio. Thus, using these multilayered compound wires, we attempted to achieve high I_c and reduce the anisotropy of J_c due to magnetic fields.

Experiment

Organic binders were added to Bi-based 2212 phase raw powder, and the resultant mixture was kneaded and turned into a slurry state. Thus, green sheets of 50~400 μm in thickness and 50 mm in width were prepared, using the doctor blade process. Then, these sheets and Ag sheets of 0.1~0.2 mm in thickness were layered. The layered sheets and Ag pipes were compounded, underwent area reduction processing, and were heat treated. Thus,the layered sheets were turned into oxide superconducting compound wire-shaped materials. This concentric multilayered compound wire-shaped material fabrication process is called the "jelly roll process." Heat treatment was carried out at temperatures ranging from 845~900°C to attain crystal orientation by melting half the Bi-based 2212 phase.

Results

Figure 1 shows an SEM image of the cross section of a fabricated multilayered compound wire-shaped material.

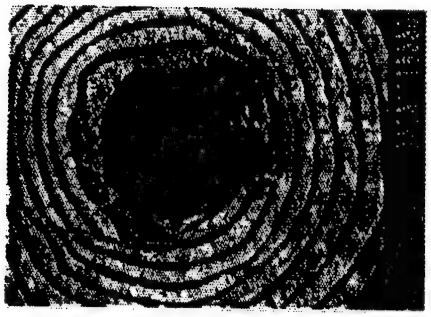

Figure 1. SEM Image of Cross Section of Compound Wire-Shaped Material

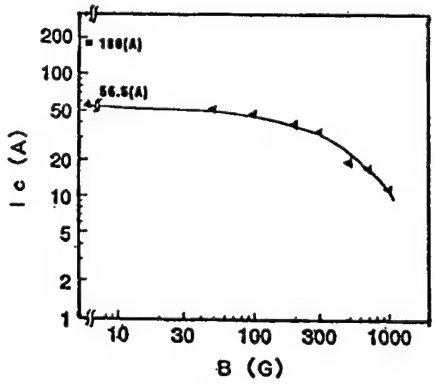

Figure 2. J_c–B Characteristics (77 K) of Compound Wire-Shaped Material

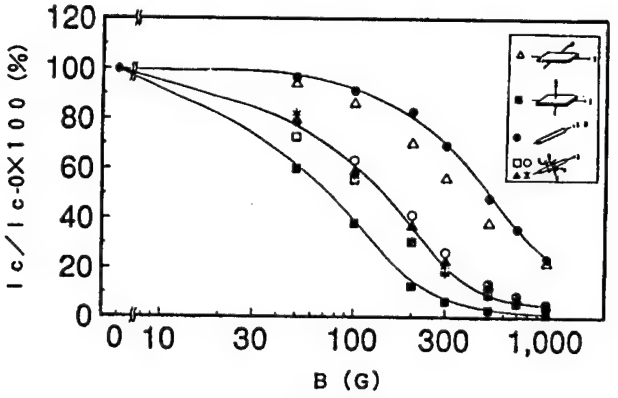

Figure 3. Magnetic Field Direction Dependence of J_c of Compound Wire-Shaped Material and Tape Wire

In the figure, the white portions show Bi-based 2212 superconducting phase, and the gray portions show silver. The number of layers is 10. We observed the orientation process of the superconducting layers of a compound wire-shaped material thus fabricated. As a result, we have found that orientation starts from the Ag sheet side and extends over the entire area as the heat treatment progresses. Figure 2 shows the magnetic field dependence of J_c of a multi-layered compound wire-shaped material, at 77 K.

I_c at 180 A shown in the figure was obtained for a tape-shaped rolled compound wire-shaped material (thickness 2 mm, width 52 mm, length 300 mm) consisting of 20 layers. Further, a comparison of the magnetic field direction dependence of J_c at 77 K was made between the compound wire-shaped material and a general tape wire. The results are shown in Figure 3. Differences resulting from magnetic field directions cannot be observed between the two types of materials. The orientation rate of the specimens shown in this figure is low, i.e., 92 percent, and, therefore, J_c lowers greatly due to magnetic field. It is thought, however, that the lowering of J_c can be improved by enhancing the orientation rate.

This research was conducted based on a contract given by the New Energy/ Industrial Technology General Organization (NEDO), as a part of the Moonlight Project "Superconducting Electric Power Application Technology Development" established by the Ministry of International Trade and Industry.

J_c Anisotropy of Bi-Based Oxide Tape

916C0018 Tokyo TEION KOGAKU CHODENDO GAKKAI YOKOSHU in Japanese 23-25 Nov 90 p 12

[Article by Hiroaki Kumakura, Kazumasa Togano, and Hiroshi Maeda, National Research Institute of Metals; Junichiro Kase, Asahi Glass Co., Ltd.; and Katsumi Nomura, Hitachi Cable, Ltd.]

[Text] **Introduction**

Bi-based oxide superconductors are high in critical magnetic field B_{c2}, and can be expected to be used as coils for superconductor magnets for generating high magnetic fields. The authors, et al., have already attempted to fabricate tape wires using the doctor blade process and Ag sheath process, and have succeeded in attaining an extremely superior critical current density (J_c) of $10^5 A/cm^2$ or larger at 4.2 K in a high magnetic field of 20 tesla or higher, as made public at the previous meeting. Not only high J_c but also small anisotropy dependence of J_c according to applied magnetic field directions play vital roles in putting the tape wires into practical use. In this research, we studied the anisotropy dependence of J_c concerning the said Bi-based oxide tape.

Experiment

Bi-based tapes composed mainly of 2212 phase were fabricated by the doctor blade process, in which the partial melting process was incorporated, and by the Ag-sheath process. All the tapes fabricated were provided with an orientation structure, in which c axes of Bi-based oxide superconductor crystal grains were lined up normal to the tape surface. Using the resistance method, J_c was measured at 4.2 K in magnetic fields up to 6 tesla, as functions of angles formed by magnetic fields and tape surface. Further, dc magnetization curves were measured at various temperatures in cases where magnetic fields were in parallel with and normal to the tape surface. Thus, the temperature dependence of J_c due to anisotropy was studied.

Figure 1 shows the angle dependence of J_c measured by the resistance method. At 4.2 K, J_c was $10^5 A/cm^2$ or larger when the magnetic flux density was 6 tesla, even when the magnetic field was normal to the tape surface, and the

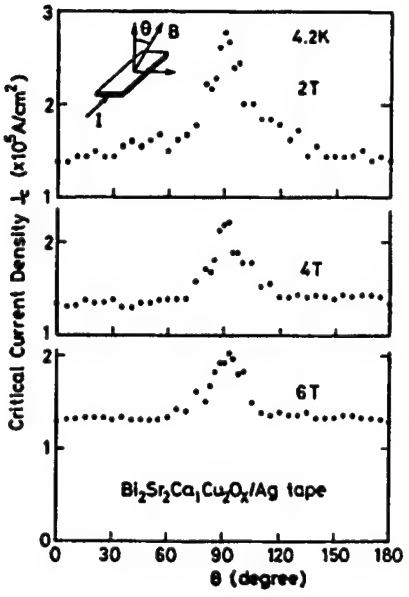

Figure 1. Angle Dependence of J_c at 4.2 K (Resistance method)

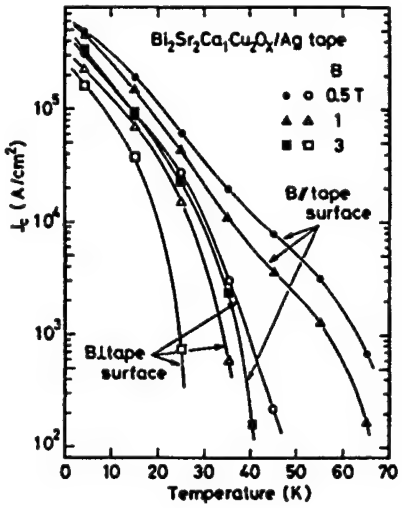

Figure 2. Temperature Dependence of J_c Obtained by dc Magnetization

anisotropic factor J_c (∥)/Jc(⊥) was small, i.e., 1.4. It has been found, therefore, that the angle dependence of J_c hardly poses problems with practical use when the tape is used at 4.2 K. This anisotropy is far smaller than that reported on thin films, etc. This is thought to arise from the uneven orientation of crystal grains of this tape material, unlike thin films. This anisotropy, however, grows rapidly as the temperature rises, as can be seen by the temperature dependence of J_c (shown in Figure 2), which was obtained by magnetization measurements.

Hysteresis Effect of J_c of Bi-Pb-Sr-Ca-Cu-O Superconducting Tape Wire

916C0018 Tokyo TEION KOGAKU CHODENDO GAKKAI YOKOSHU in Japanese 23-25 Nov 90 p 13

[Article by Shouji Otabe and Teruo Matsushita, Information Engineering Department, Kyushu Technical College; Sakae Kodahara, Engineering Department, Kyushu University; and Takeshi Hikata and Kenichi Sato, Sumitomo Electric Industries, Ltd.]

[Text] **1. Introduction**

The critical current density J_c of Ag-sheathed BiPbSrCaCuO superconductors prepared by the powder-in-the-tube process shows high values because of the good intercrystal grain bonding.[1] Thus, by using materials with high J_c, current leads, multicore wires, coils, etc., have already been fabricated on a trial basis.[1] Meanwhile, the hysteresis effect of J_c is being observed. It can be said, therefore, that J_c can be further increased by strengthening the bonding between crystal grains. In this research, we intend to study J_c during cooling in a magnetic field (FC), as well as in the process of magnetization and demagnetization, in order to study the hysteresis effect of Bi-based specimens.

2. Experiment

Bi_2O_3, PbO, $SrCO_3$, $CaCO_3$, and CuO powders were used as raw materials to prepare specimens. These powders were calcined, sintered, pulverized, and put in an Ag sheath which, in turn, was drawn in the form of round wire. Then, the round wires were further rolled in the form of tape. The size of the specimens thus prepared ranged from 2.5~4.5 mm in width, and 0.1~0.2 mm in thickness.

The J_c of the specimens was measured at temperatures ranging from 4.2~20 K in an He gas atmosphere. The error of each temperature was controlled within 0.5 K. The micro alternating-current magnetic field superimposed method (ac method) was used to measure J_c. The dc and ac magnetic fields were applied in parallel with tapes. Therefore, J_c measured was a mean value of J_c inside the a-b plane and J_c in the c-axis direction. However, since the thickness of the tapes was small, J_c in the a-b plane is thought to have been strongly reflected. The frequency of the ac magnetic field was 35.0 Hz.

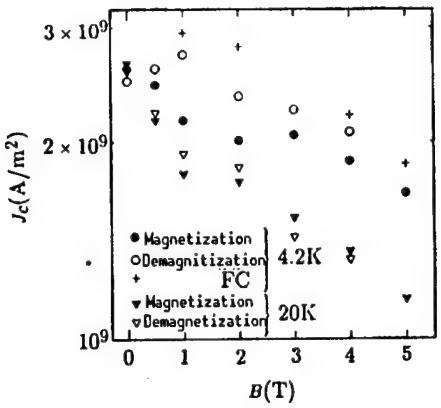

Figure 1. Magnetic Field Dependence of J_c of Specimens

To reduce the effect of shielding current in grains on weak links, we measured J_c during FC. A magnetic field was applied to the specimens during FC at temperatures higher than T_c, and the temperature of the specimens was lowered. Thus, the specimens were placed in a superconducting state, and their J_c was measured. In this case, magnetic flux is trapped in the specimens and, therefore, the shielding current in grains amounts to nearly zero. It is thought, therefore, that J_c nearly midway between magnetization (in which J_c is low by strengthening the effect of weak link) and demagnetization (in which J_c is high by weakening the effect of weak link) is obtained.[2]

3. Results and Discussion

Figure 1 shows J_c during magnetization and demagnetization at 4.2 K and 20 K, respectively. J_c at 4.2 K was not as affected by the magnetic field and did not decrease, where J_c at 20 K decreased with the application of a magnetic field. No large hysteresis effects could be observed, since J_c values were comparatively large. Hysteresis effects, however, still remained at 4.2 K. Meanwhile, the effect of magnetic field was little observed at 2 K. The results of FC were seen for J_c at 4.2 K. These values were larger than those in demagnetization. This is estimated to have resulted from the upper limit of the magnetic field applied being low, i.e., 5 T during demagnetization and J_c not having completely returned to the major curve.

References

1. Sato, K., et al., Applied Superconductivity Conference, Snowmass, 1990.

2. Matsushita, T., et al., "Adv. Superconductivity," Springer, Verlag, Tokyo, 1989, p 393.

Distortion Effect of Ag-Sheathed Bi-Based Superconducting Tape (2)

916C0018 Tokyo TEION KOGAKU CHODENDO GAKKAI YOKOSHU in Japanese 23-25 Nov 90 p 14

[Article by Keisuke Yamamoto and Junichi Kai, Central Research Laboratory, Mitsubishi Cable Industries Co., Ltd.]

[Text] **1. Introduction**

Ag-sheathed Bi-based superconducting wires can be processed into tapes by rolling and pressing. Thus, the formation of fine crystals and orientation can be facilitated, and a high J_c of $10^4 A/cm^2$ (at 77 K) has been obtained. It can be said that if the range of application is narrowed, superconducting wires are considerably near the practical use level. We, therefore, are conducting experiments of almost practical use level, such as preparation of longer wires and coils. One characteristic posing problems, however, is the deterioration of J_c when mechanical distortions are given to tapes. At the last meeting, we reported on the characteristics of tapes against tensile distortions.[1] In this study, we measured the bending distortion of tape specimens (prepared under various conditions) using the W&R method, and report on the results.

2. Experiment

Using the general powder-in-tube process, we prepared nine types of Ag-sheathed Bi-based superconducting tapes (thickness: 0.15~0.2 mm; width: 2.6□3.0 mm; length 40~41 mm) by changing three types of charge composition ratios (Bi:Pb:Sr:Ca:Cu = (I) 8:2:10:10:15, (II) 9:2:10:11:15, and (III) 10:2:10:10:15), and three types of heat treatment and press conditions {S(160), S(160)+P+S(40), S(160)+P+S(40)+P+S(40); S: sintering, ( ) hours at 830~840°C, P: pressing at 2 x 10^3MPa).

Under the W&R method, we measured I_c of these tapes at zero magnetic field in liquid nitrogen, while applying bending distortions (0~1 percent) to each tape. The dc four-probe method was used to measure I_c, and the definition was 1 μV/cm. A cross sectional area obtained by removing the Ag-sheathed portion from the total cross sectional area of each tape, was used to calculate J_c. The longitudinal cross section of each tape was observed by SEM, after the measurement of the effect of distortion.

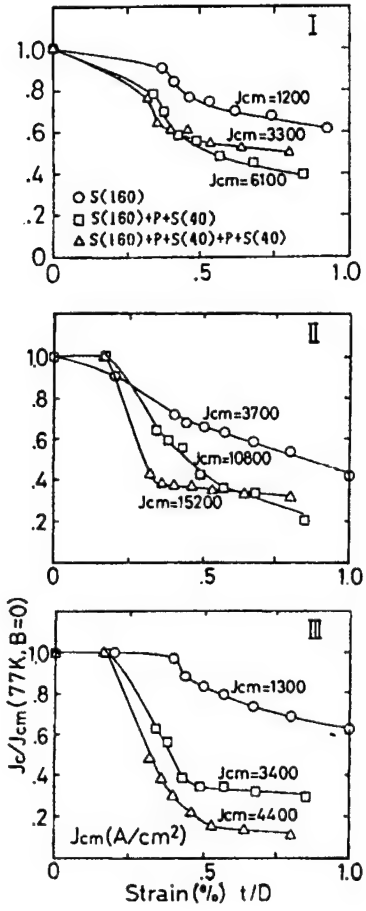

Figure 1. Bending Distortion Dependence of J_c

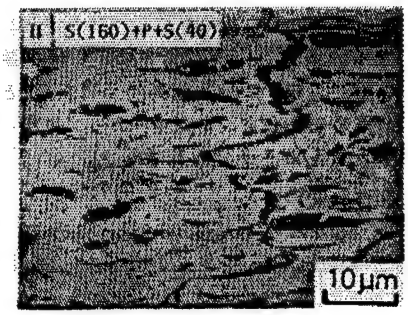

Figure 2. SEM Image of Tape Longitudinal Section After Measurement of Effect of Bending Distortion

3. Results

Figure 1 shows the bending distortion dependence of J_c. Each tape was able to maintain J_c that was more than 90 percent of J_{cm} (J_c in the case of 9 percent distortion) when distortions of up to about 0.25 percent were applied. Each tape, however, showed a rapid deterioration of J_c when distortions of 0.3 percent or larger were applied. It can be seen that the degree of deterioration of J_c depends on the specimen preparation conditions. One such condition is charge composition ratio. In other words, the degree of deterioration of J_c lowers in the order of charge composition ratios I, II, and III. Further, the degree of J_c deterioration of the tapes not intermediately pressed is small compared with the tapes intermediately pressed. These two different trends appear to be associated with the types, quantity, and size of nonsuperconducting crystal grains, which result from different charge composition ratios, and with the refining and orientation of superconducting crystal grains obtained by intermediate press treatment.

Figure 2 shows an SEM image (BEI) of the longitudinal section of a typical tape after measurement of the effect of distortions. Cracks thought to be a major cause of deterioration of J_c can be observed.

References

1. Yamamoto, K., et al., "Cryogenic Engineering," Engineering Society Meeting, preliminary draft, 1990 spring term, p 220.

Superconducting Materials for Magnetic Bearings

916C0018 Tokyo TEION KOGAKU CHODENDO GAKKAI YOKOSHU in Japanese 23-25 Nov 90 p 45

[Article by Makoto Okano and Toshitada Onishi, Electronic Technology Research Laboratory; and Masato Murakami, Naomi Koshizuka, Ouji Koyama, Hiroyuki Fujimoto, Toru Shiobara, and Shoji Tanaka, Superconductivity Engineering Research Laboratory]

[Text] **1. Introduction**

Using high temperature oxide superconductors, we are studying whether superconducting magnetic bearings can be put into practical use on an industrial scale. In this research, we measured bearing performance for the conventional metal-based superconductor Nb, NbTi, and for the oxide superconducting material $Y_1Ba_2Cu_3O_x$ (YBCO) prepared by the melt extraction process (MPMG process). Thus, we conducted comparative studies on these materials as bearing materials.

2. Testing Equipment and Test Results

Figure 1 shows an outline of the bearing performance measuring equipment. Experiments were conducted in liquid helium, and in liquid nitrogen when oxide superconductors were used. The number of windings in the coils was 1,500. A load was applied to specimens from the room temperature via a stainless rod, and displacement in this case was measured by the micrometer head to obtain the floating performance.

Figure 2 shows the results of measurement of floating rate at the liquid helium temperature. In the figure, thick solid lines show the values obtained by analyzing superconductors as complete diamagnetic substances. Calculated values on Nb with high H_{c1} or YBCO with strong pinning force show a highly satisfactory conformance with actual measured values. In particular, with respect to YBCO with high H_{c2} and J_c, a high load capacity was obtained. It is expected, therefore, that performance equivalent to conventional noncontact bearings on an industrial scale can be obtained. Data is only available up to 2 A at the liquid nitrogen temperature, but actual measured values considerably lowered calculated values. The intrusion of magnetic fields into

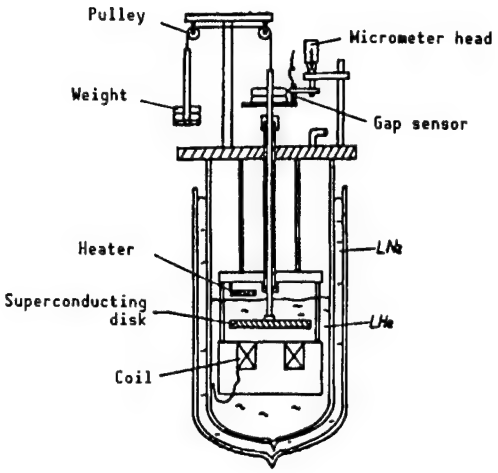

Figure 1. Performance Measuring Equipment

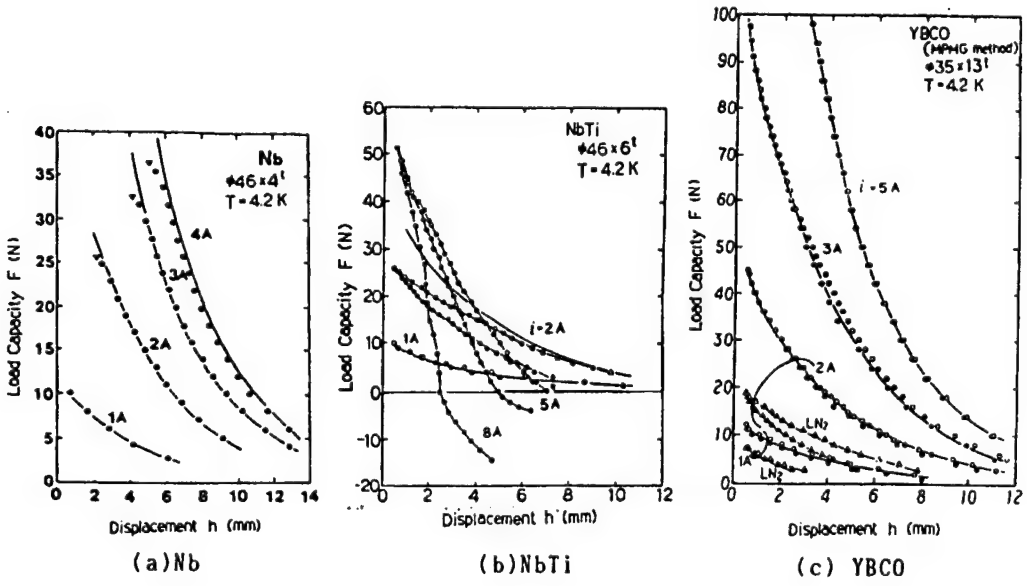

Figure 2. Floating Performance of Various Superconducting Materials

the bulk appears to be large. In the case of NbTi, the intrusion of magnetic fields into the bulk is large at 2 A or more, and creep phenomenon also seems to occur.

Magnetic Bearing Using High-Temperature Oxide Superconductor (III)

916C0018 Tokyo TEION KOGAKU CHODENDO GAKKAI YOKOSHU in Japanese 23-25 Nov 90 p 46

[Article by Ryoichi Takahata, Koyo Seiko Co., Ltd.; and Masashi Yotsuya, Osaka Prefectural Industrial Technology Research Laboratory]

[Text] **1. Introduction**

Using the diamagnetic characteristics of superconductors, we fabricated bearings for trial, and have found that floated rotors stably rotate but that the flotation power is small. We have already reported on these results.[1] Meanwhile, the critical current density J_c of Y-based superconductors has recently been improved by the new melt extraction process (quench and melt growth (QMG) process).[2] The use of Y-based superconductors is thought to make it possible to improve the floating power. For this study, therefore, we prepared superconductors using the QMG process in order to apply them to bearings. Then, we compared the superconductors prepared by the QMG process with those prepared by the solid phase reaction process (SR process) with regard to their magnetic force.

2. Experiment

Figure 1 shows a unit[3] used to measure the repulsive force of a permanent magnet that floats on the superconductor. This unit measures the force acting on the permanent magnet, using a distortion gauge located on the plate spring installed on the permanent magnet.

One end of the plate spring provided with a permanent magnet is fixed on a single axle stage; this plate spring can be driven, by motor, on the superconductor. The relative distance between the superconductor and permanent magnet was measured by a laser displacement measuring system. The permanent magnet was 4 mm in diameter and 2 mm in length and weighed 0.2 g in volume. Figure 2 shows a magnetic field distribution of the permanent magnet.

The plate spring was made of aluminum, and was 1.0 mm thick, 7 mm wide, and 180 mm long. This plate spring with a permanent magnet was moved vertically and horizontally on the superconductor surface, and force acting on the permanent magnet was measured using a distortion gauge.

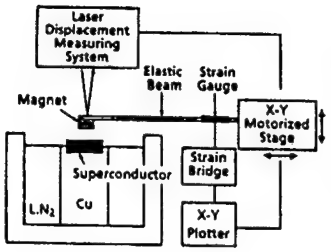

Figure 1. Repulsive Force Measuring Unit

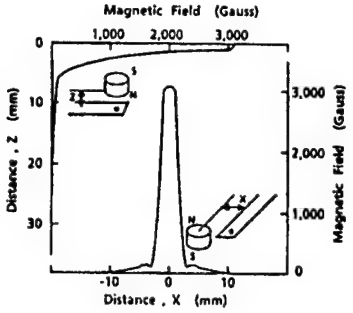

Figure 2. Magnetic Field of Permanent Magnet

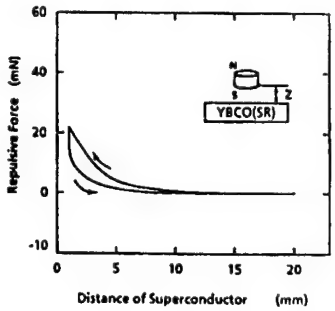

Figure 3. Magnetic Repulsive Force of Superconductor Prepared by SR Process

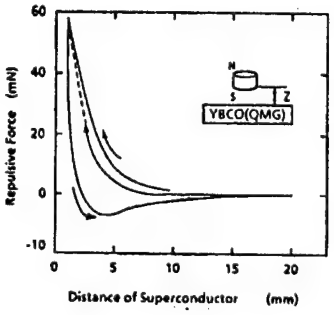

Figure 4. Magnetic Repulsive Force of Superconductor Prepared by QMG Process

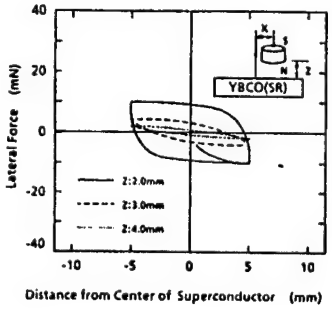

Figure 5. Magnetic Resistance of Superconductor Prepared by SR Process

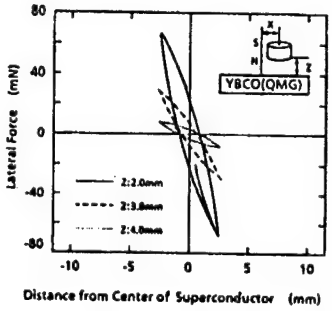

Figure 6. Magnetic Resistance of Superconductor Prepared by QMG Process

The specimens used were $YBa_2Cu_3O_x$ (ϕ18.5 x 3.5) and $YBa_2Cu_3O_x$ (ϕ17.5 x 8.0) prepared by the SR and the QMG processes, respectively.

3. Results and Discussion

Figures 3 and 4 show the results of the measurement of magnetic repulsive force at the vertical distance between the superconductors (prepared by the SR and QMG processes) and the permanent magnet.

Magnetic force (rigidity) of the permanent magnet (put on each superconductor) at the lateral distance was also measured. The results are shown in Figures 5 and 6.

In every case, a hysteresis was present in the magnetic force (of the superconductors) that acts on the reciprocating motion of the permanent magnet. It has been found that repulsive force and rigidity is larger in superconductors prepared by the QMG process than in those prepared by the SR process.

This is thought to result from the superconductors prepared by the QMG process having a large flux pinning force. Superconductors prepared by the QMG process, therefore, appear to be very effective for application to bearings.

References

1. Takahata and Yotsuya, 1990 Spring Cryogenics Engineering Superconductor Society Meeting Preliminary Draft

2. Murakami, et al., JPN. J. APPL. PHYS., Vol 28, 1989, p 1189.

3. Moon, et al., APPL. PHYS. LETT., Vol 52 No 18, 1988, p 1534.

Measurement of Drag Force, Floating Power by Magnetic Flux Penetration in Ceramic Superconductors

916C0018 Tokyo TEION KOGAKU CHODENDO GAKKAI YOKOSHU in Japanese 23-25 Nov 90 p 47

[Article by Yoshihiko Maeda and Kazuyuki Aihara, Tokyo Electric College; and Hiroyuki Fujita, Industrial Technology Research Laboratory, Tokyo University]

[Text] **1. Introduction**

Research called "micromechatronics," in which actuators of μm order are manufactured using the semiconductor process technology for integrated circuits, has recently been conducted.[1] However, there are problems with micromechatronics. One of them is friction force acting on the portion where moving parts come into contact with fixed parts. To resolve this problem, we fabricated actuators that float moving parts using the superconductor Meissner effect.[2] However, ceramic superconductors (hereinafter referred to as "superconductors") cause magnetic flux to penetrate the inside. If magnetic flux attempts to move, drag force to prevent such movement of magnetic flux occurs. In this research, we measured drag force, using a spring that acts when a yttrium-based (hereinafter referred to as "Y-based") superconductor, a bismuth-based (hereinafter referred to as "Bi-based") superconductor, and a magnet (located 1~15 mm away from these superconductors) carry out relative motions. Further, we measured repulsive force using the same magnet, and studied the relationship between drag force and repulsive force.

2. Experiment

Figure 1 shows a general view of the drag force measuring unit. Drag force acting on the magnet located 1~15 mm away from the superconductor was measured using a spring, by rotating the superconductor. In this case, the drag force was assumed to be a force applied to the end of the magnet. Measurements were carried out using three types of superconductors (two types of Y-based superconductors that are different in thickness, and a Bi-based superconductor) and two types of magnets (cylindrical ($9 \times 4 \times 5$ mm^3) and discoid ($25\pi \times 5$ mm^3)), by changing the speed of rotation (100/3 rpm, 45 rpm). Thus, changing the measuring conditions, we investigated the effect of thickness and construction material on drag force, the effect of differences in superconductor surface

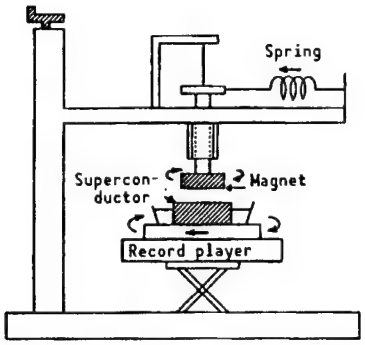

Figure 1. Drag Force Measuring Unit

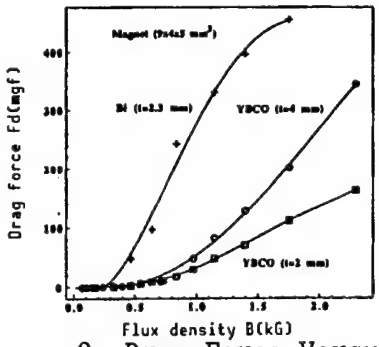

Figure 2. Drag Force Versus Flux Density

magnetic flux density on drag force, and the rotating speed dependence of drag force.

Further, we measured the floating height by adding a weight to the magnet used to measure drag force. Thus, we measured the repulsive force and investigated the relationship between the repulsive force and drag force.

- Superconductors

  · Y based (No. 1): Dimensions (diameter: ϕ25 mm, thickness: 2 mm)
  Characteristics of construction material (T_c = 90 K, J_c = 210 A/cm^2; H_{c1} = 12.50 O_e)

  · Y based (No. 2): Dimensions (diameter: ϕ25 mm, thickness: 4 mm)
  Characteristics of construction material (same as those of No. 1)

  · Bi-based: Dimensions (area: 17 x 17 mm^2, thickness: 2.3 mm)
  Characteristics of construction material (T_c = 105 K, J_c = >1,000 A/cm^2; H_{c1} = 18.2 O_e)

3. Results and Discussion

We measured the repulsive force and drag force by changing the shape of the magnet. Where the magnet was discoid, the drag force was so small as not to have been detected. Further, since there was no large difference in the two types of speed of rotation, the speed dependence of drag force was not detected in this research.

Figure 2 shows drag force versus magnetic flux density. As flux density increases, drag force grows. The Y-based superconductor curves show that the thicker the superconductor, the larger the drag force. This is thought to result from the long flux penetration route inside the superconductor causing a large drag force. The Bi-based superconductor curve shows that the drag force tends to saturate as flux density grows. This is thought to result from the pinning force (causing drag force) weakening due to decreased superconducting area inside the superconductors.

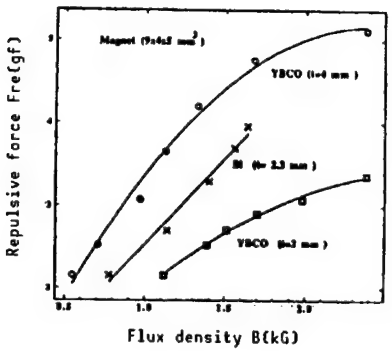

Figure 3. Repulsive Force Versus Flux Density

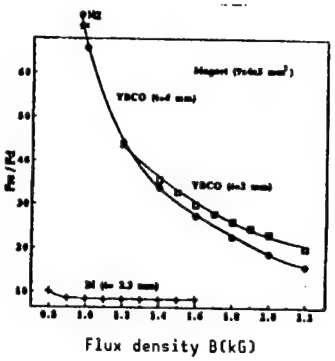

Figure 4. Repulsive Force/Drag Force Versus Flux Density

Figure 3 shows repulsive force versus flux density. Figure 4 shows the ratios of the repulsive force to the drag force (F_{re}/F_d) obtained from Figures 2 and 3. From Figure 4, the following can be shown: The F_{re}/F_d of the Bi-based superconductor tends to become constant as the flux density increases. The F_{re}/F_d of the two types of Y-based superconductors shows a tendency to decrease as the flux density grows. Thus, these two F_{re}/F_d come close to each other. When the flux density is 1.2 kG, the F_{re}/F_d of Y-based superconductors amount to five times that of the Bi-based superconductor.

4. Conclusion

We measured drag force and repulsive force involved with flux penetration, and investigated the relationship between these types of force. The measurement of drag force showed that if the density of flux applied to superconductors remains constant, no drag force occurs. Further, the drag force of the Bi-based superconductor showed a tendency to saturate. As the flux density increased, the ratio of drag force to repulsive force became as follows:

- Bi-based superconductor: Remained constant
- Y-based superconductor: Decreased

References

1. Fujita, Electrical Society Thesis D, Vol 108, 1988, p 205.

2. Kin, Katsurai, and Fujita, 1990 Electrical Society All-Japan Meeting Collection of Lectures, 8, pp 87-88.

Large Magnetic Floating Force of YBaCuO Prepared by MPMG Method

916C0018 Tokyo TEION KOGAKU CHODENDO GAKKAI YOKOSHU in Japanese 23-25 Nov 90 p 48

[Article by Masato Murakami, Tomoji Koyama, Horiyuki Fujimoto, Satoshi Goto, Toru Shiobara, Naomi Koshizuka, and Shouji Tanaka, Superconductivity Engineering Research Institute]

[Text] **1. Introduction**

As applications for superconductors, bearings using the magnetic repulsive force, magnetic flotation transportation equipment, etc., have already been proposed. The magnetic flotation force of oxide superconductors, however, is not so large, and large flux creeps occur at high temperatures. The application of superconductors at the liquid nitrogen temperature, therefore, is deemed to be considerably difficult. Preparation of bulk materials with comparatively high flux pinning force enables large flotation force to be obtained, resulting in small flux creep. This report presents the preparation process and characteristics of bulk superconducting materials that exhibit large magnetic repulsive force.

2. Experiment

Using the MPMG process,[1] we fabricated oxide superconductors. To prevent macrocracks, however, we melted the raw materials and added silver oxide to the melted raw materials in the process of pulverization and mixing, so that silver particles can be dispersed to the matrixes. With respect to the floating power, we investigated the relationship between the distance and generating power, while bringing a magnet of about 2.5 cm in diameter closer to a bulk material of about 3.5 cm in diameter and 2 cm in height.

3. Results and Discussion

Figure 1 shows a change in the structure of YBaCuO fabricated by the MPMG process, adding silver. The figure shows that macrocracks are apparently reduced. Thus the dispersion of Ag makes it possible to control the propagation of cracks and to improve the magnetization (M) per unit volume, thereby serving to enhance the flotation force ($F = MdH/dz$).

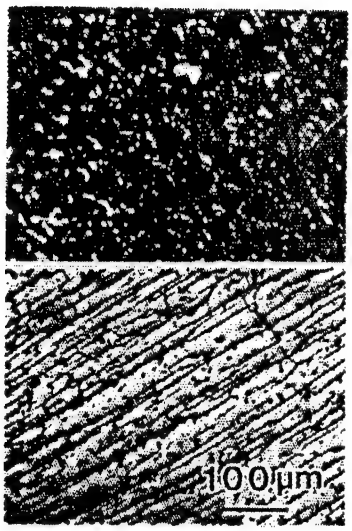

Figure 1. Structural Change Due to Addition of Ag

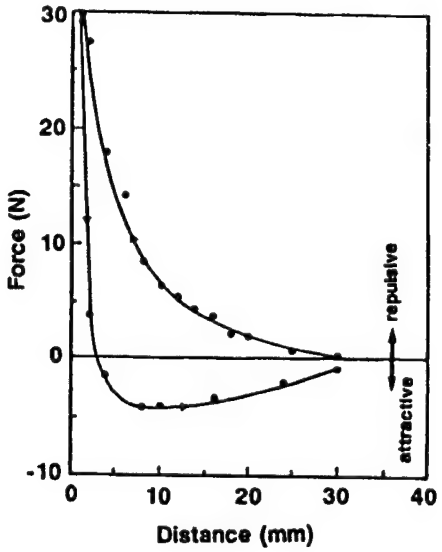

Figure 2. Relationship Between Flotation Force and Distance

Figure 2 shows the relationship between the flotation force and distance for YBaCuO (to which Ag was added by 10 mass percent at 77 K. The flotation force was improved by narrowing the distance, and became 30 N at 1 mm. From this point, when the magnet was kept away from the bulk material, the flotation force rapidly decreased and became an attractive force from a certain distance. This phenomenon can be explained by the distribution of flux inside superconductors.

References

1. Fujimoto, H., et al., Proc. ISS 89, p 285.

Current Lead Using Bi-Based Oxide Superconductor (2nd Report)

916C0018 Tokyo TEION KOGAKU CHODENDO GAKKAI YOKOSHU in Japanese 23-25 Nov 90 p 111

[Article by Tomoyuki Yanagiya, Tomoya Narita, Yutaka Yamada, Junji Sakuraba, and Mamoru Ishihara, Hiratsuka Research Laboratory, Sumitomo Heavy Industries, Ltd.]

[Text] **1. Introduction**

In the previous report,[1] we reported that the amount of heat penetrating from outside can be greatly reduced by using oxide superconductors with small heat conductivity as current leads. In this research, we electrified oxide superconductors up to 140 A, and measured the amount of penetrated heat.

2. Experiment

(1) Preparation of Superconductor Bulk

As described in the previous report, Bi-based superconducting powder (prepared by the solid phase reaction process) was formed using cold isostatic pressing (CIP). The formed powder was sintered, and bulks of 300 mm each in length and 7 mm each in diameter were obtained. CIP and sintering were repeated twice.

(2) Evaluation of Amount of Penetrating Heat

The amount of heat that had penetrated into the superconductor bulks was measured by using a cryostat fabricated for trial. Two bulks were installed on the measuring unit, and their lower ends were connected to each other with NbTi wire (Figure 1). The upper ends of the specimens were cooled with liquid nitrogen, and the lower ends were immersed in liquid helium. The amount of heat that had penetrated into the superconductor bulks was obtained by measuring the evaporation of liquid helium.

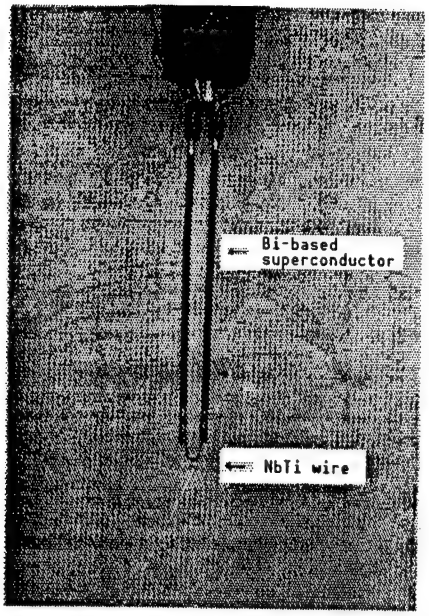

Figure 1. Appearance of Specimen

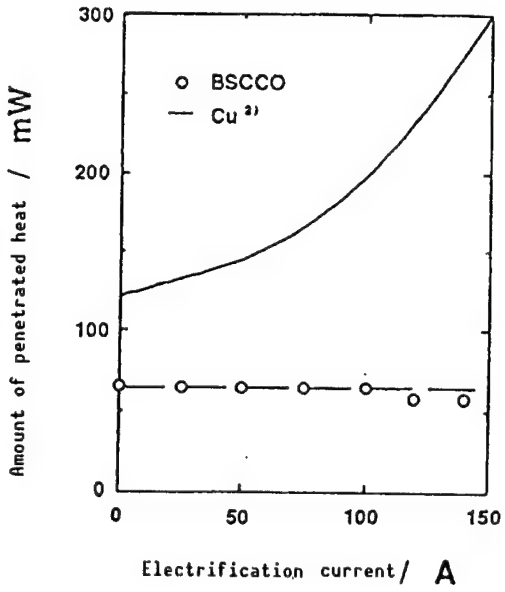

Figure 2. Relationship Between Electrification Current and Amount of Penetrated Heat

3. Results

The upper ends and lower ends of the superconducting specimens installed as per Figure 1 were maintained at 68~70 and 4.2 K, respectively. The distance between the lower ends and upper ends was 17~18 cm. Figure 2 shows the relationship between the electrification current and amount of penetrated heat when the current was changed from 0 to 140 A.

In the case of the oxide superconductors, the amount of penetrated heat changed little and ranged from 55~65 mW, even though the current increased. The solid line in the figure shows an example of the relationship between the electrification current and amount of heat penetrated for a copper gas-cooled current lead of the 100 A class.[2] The amount of heat that had penetrated into the oxide superconducting current lead was about one-half at 0 A and about one-third at 100 A, of the copper current lead.

References

1. Yanagiya, et al., 43rd 1990 Spring Cryogenics Engineering/Superconductivity Society Meeting, C2-12.

2. Efferson, K.R., REV. SCI. INSTR., Vol 38, 1967, p 1776.

Heat Load Characteristics of Y-Based Superconductor Electrode Joint

916C0018 Tokyo TEION KOGAKU CHODENDO GAKKAI YOKOSHU in Japanese 23-25 Nov 90 p 112

[Article by Masahiko Sano, Akihiko Kawashima, Makoto Seki, Susumu Ozawa, Hiroshi Yamamoto, and Shouichi Tanaka, Engineering Department, Nippon University; and Youichi Matsubara and Takeshi Ogasawara, Nuclear Research Laboratory, Nippon University]

[Text] **1. Introduction**

High temperature oxide superconductors have low heat conductivity at temperatures less than the critical temperature, and do not generate Joule heat. Therefore, we are studying the application of high J_c Y-based superconductors (fabricated by the MPMG process) to refrigerator-cooled current leads. This report describes heat conductivity in a superconducting state, and the results of experiments when currents were applied to specimens up to 100 A. Further, on the basis of the results of experiments, we simulated the heat generating condition during the quenching of YBCO current leads.

2. Experiment

We separately reported on the details of the heat conductivity measuring method.[1] For the electrification experiments, the YBCO (prepared by the MPMG process) was formed into a rectangular parallelepiped of several mm square. Ag was evaporated on the electrode joint, Ag paste was further doped on the joint to obtain a good contact, and the joint was annealed. Thus, the quench current was measured by plotting the voltage-current characteristics while current was being applied up to 100 A by changing the sweep speed.

3. Results and Discussion

Figure 1 shows the results of thermal conductivity. At temperatures ranging from 10~50 K, the thermal conductivity was several tenths of that of phosphorous deoxidized copper so far used for current leads.

The results of electrification are as shown in Figure 2. The results show that current can be applied up to 83 A at 26 K.

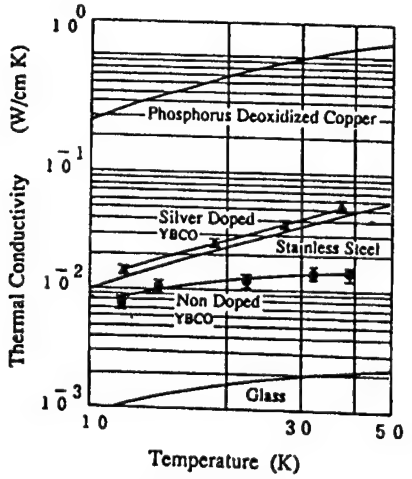

Figure 1. Thermal Conductivity of YBCO

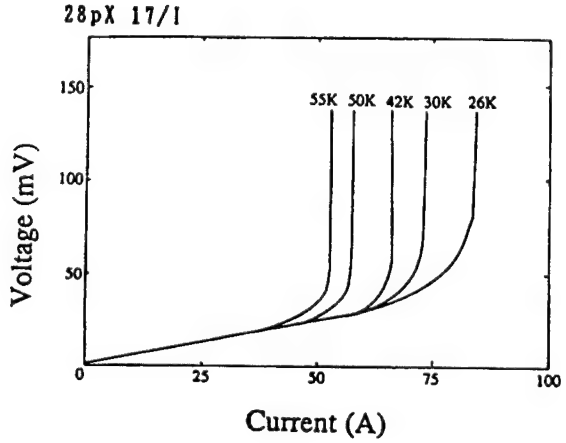

Figure 2. Results of Electrification

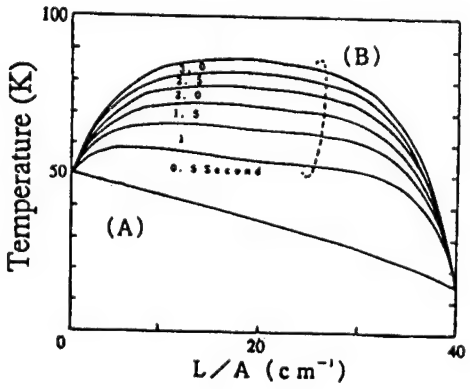

Figure 3. Temperature Distribution During Electrification of Overcurrent

We simulated a temperature distribution in the longitudinal direction of the YBCO specimen where there was a difference in temperature between both ends of the specimen, that is, 50 K and 15 K, while assuming current lead. The results are as shown in Figure 3. The YBCO specimen was 4 cm in length, 8 mm^2 in sectional area. In this case, the quench current was 1 A. The figure shows that the specimen is placed in a superconducting state at current values before the quench current becomes 17 A and that the lead temperature distribution remains (A). However, when the quench current becomes 17 A, the superconducting state collapses, Joule heat is generated, and the temperature of the current lead rises (B). The interval between leads is 0.5 seconds. It can be seen that the temperature reaches the nitrogen temperature in two seconds. The details will be reported at the meeting.

References

1. Sano, et al., 37th Appl. Physics Association Lecture Meeting, Spring 1990.

Oxide Superconducting Current Lead

916C0018 Tokyo TEION KOGAKU CHODENDO GAKKAI YOKOSHU in Japanese 23-25 Nov 90 p 113

[Article by Koichi Numata, Kazuhiko Kato, Kazutomo Hoshino, and Hidefusa Takahara, General Research Institute, Mitsui Mining and Smelting Co., Ltd.]

[Text] **Purpose**

The method of connecting current poles poses large problems in the application of oxide superconductors, irrespective of whether the application field is strong or weak current. For this research, in particular, it is necessary to flow currents of several hundreds to kA order inside current leads. Unless the connection resistance is reduced, the practical use of current leads cannot be achieved, however greatly the critical current of oxide superconductors is improved. Many papers have already been published concerning problems with connection resistance. A connection resistance of $10^{-10}\Omega \cdot cm^2$ has been reported[1]; however, this was a case where small current was applied to a small sample; no paper describes the case where large current was applied.

In this research, a small connection resistance of $10^{-5}\Omega \cdot cm^2$ or less was obtained by using a comparatively simple process in which Ag foil is solderless contacted. The characteristics of the connection resistance are reported below.

Experiment

Coprecipitated powder with a composition of Bi:Pb:Sr:Ca:Cu = 0.8:0.2:0.8:1.0:1.4 (mole ratio) was calcined, and Bi-based high T_c phase powder was obtained. The powder was uniaxially pressurized and formed (300 kg/cm^2) into a disk 20 mm in diameter and 2 mm in thickness, and further underwent cold isostatic pressing (CIP) (1 ton/cm^2). This specimen was heat treated at 845°C for 24 hours, and cut to a small rectangle of 3 mm in width. Then, Ag foil of 20 μm was solderless contacted 3 mm wide on both ends of the rectangle (Figure 1).

The specimen obtained was sintered at 845°C for 24 hours and was used for measurement. Further, a rod-shaped specimen of 15 mm in diameter and 150 mm in length was prepared in the same process as that for the disk-shaped specimen, and the connection resistance was measured.

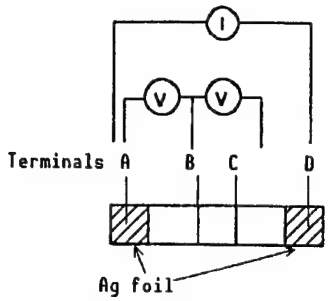

Figure 1. Connection of Terminals to Specimen

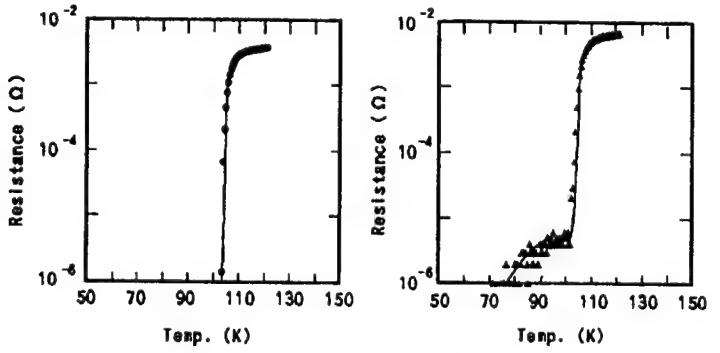

Figure 2. Results of Measurement of Critical Temperature and Connection Resistance

Four terminals were provided to measure the critical temperature and critical current. The three-terminal method was used to measure the connection resistance. A current was applied between terminals A and D, and potential differences between terminals A and B were measured (Figure 1).

Results

Figure 2 shows the temperature dependence of connection resistance. • shows a transition curve of the specimen measured by the four-terminal method, and ▲ shows the temperature dependence of connection resistance measured by the three-terminal method. The critical temperature of this specimen is 103 K. The results of measurements at temperatures lower than 103 K, using the three-terminal method, show the temperature dependence of connection resistance values. $dR/dT > 0$, and, therefore, the temperature dependence of this connection resistance is metallic; the connection resistance is about $10^{-6}\Omega \cdot cm^2$ at 77 K.

We are currently measuring changes in connection resistance values when a current of about 100 A is applied to the rod-shaped specimen and will report on the results at the meeting.

References

1. Ekin, J.W., et al., APPL. PHYS. LETT., Vol 52, 1988, p 1819.

Current Control Superconducting Switch

916C0018 Tokyo TEION KOGAKU CHODENDO GAKKAI YOKOSHU in Japanese 23-25 Nov 90 p 114

[Article by Hiroshi Sato, Harufumi Kondo, and Osami Tsukamoto, Engineering Department, Yokohama National University]

[Text] **1. Introduction**

High temperature oxide superconductors are characterized by their large nonsuperconducting resistance. In addition, processing them into thin films makes it possible to increase the area that comes into contact with the refrigerant. High temperature oxide superconductors, therefore, are materials suitable for operating superconducting switches at high speed. We are currently conducting research on superconducting switches using these oxide materials. To turn off superconducting switches, we employed the method of adding pulse overcurrent.

2. Experiment

The sample was a rectangular Y-based oxide superconductor, and J_c was about $5 \times 10^6 [A/cm^2]$.

With respect to the test circuit, the sample was connected to the power supply in series, and a hole device to measure current was inserted between the sample and the power supply. The power supply was feedback controlled, so that the hole device output voltage could be equalized to the personal computer D/A board output reference signals. The current waveform was of a three-stage pulse structure. The first, second, and third stages are herein called "stationary operation current," "pulse overcurrent," and "residual current," respectively. The third stage residual current was used for measurement after the pulse overcurrent was cut off.

Hole device output voltage and voltage at both ends of the sample were measured by a transient recorder.

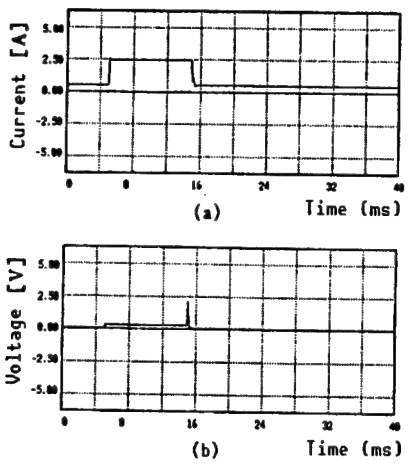

Figure 1. Switching Characteristics
(a) Current waveform
(b) Voltage waveform

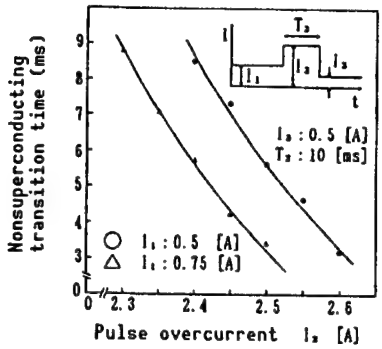

Figure 2. Nonsuperconducting Transition Characteristics

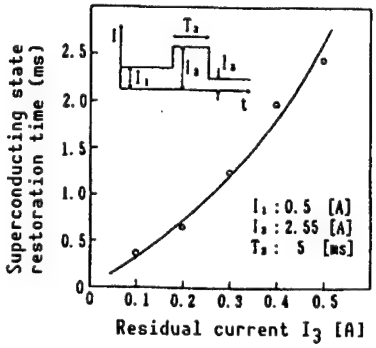

Figure 3. Superconducting State Restoration Characteristics

3. Results and Discussion

Figure 1 shows an example of results of experiments. The current waveform (a) shows that the current became almost constant by the feedback control. The voltage waveform (b) shows that the voltage was nearly zero while stationary operation current and residual current were being applied, but that the voltage rapidly rose when the application of pulse overcurrent was about to be finished. This is thought to result from the following:

(1) Superconducting and nonsuperconducting states mixedly exist for some time immediately after the application of pulse overcurrent.

(2) The entire sample is quenched, due to the effect of heat generated and other factors, just before the completion of pulse overcurrent application.

Next, we investigated the time until the entire sample was quenched, that is, the superconducting switch became off. The results are as shown in Figure 2.

The time required for transition to the nonsuperconducting state was considerably short, that is, several ms or less. Figure 2 also shows that the time required for transition to the nonsuperconducting state depends on the

stationary operation current. This appears to be caused by the generation of heat due to the sample's contact resistance.

We also investigated the time until the sample was again restored to the superconducting state after pulse overcurrent was cut off, and obtained the results shown in Figure 3. From the figure, it is clear that the sample can be restored to the superconducting state at considerably high speeds.

As a result, it has been clarified that an appropriate selection of stationary operation current and residual current makes it possible to operate superconducting switches at high speeds.

4. Conclusion

We have been able to confirm that superconducting switches can be controlled and operated using current. We have also found that the time until superconducting switches become OFF depends on the size of the stationary operation current and the pulse overcurrent, and that the time until the switches again become ON depends on residual current.

These results show that an optimum selection of stationary operation current, pulse overcurrent, and residual current may make it possible to develop switching devices to cope with 50/60 Hz.

References

1. Sato, Michishita, and Tsukamoto, 43rd Cryogenics Engineering/Superconducting Society Meeting Preliminary Draft Collection, 1990, p 221.

2. Sato and Tsukamoto, Electrical Society Static Equipment Research Meeting Data, 1990, p 1.

Effect of Light Irradiation on Bi-Based Superconductor V-I Characteristics

916C0018 Tokyo TEION KOGAKU CHODENDO GAKKAI YOKOSHU in Japanese 23-25 Nov 90 p 115

[Article by Noriyuki Shimizu and Tatsuichi Yoshida, Engineering Department, Nagoya University; Akira Saji, Chubu Electric Power Co., Inc.; and Noriya Horii, Toyoda Technical College]

[Text] **Introduction**

When constant current is applied to the superconducting coils of superconducting electrical equipment such as superconducting magnetic energy storage (SMES) systems, and this current is held (permanent current mode) in the coils, provided the coils are short-circuited by the superconductors, no energy loss will occur. Superconducting switches so far developed for the above purpose use thermal, magnetic field, and mechanical contacts as triggers for switch on and off, and are slow in operating speed. Therefore, for equipment requiring speedy on-off switching, current is controlled by semiconductor devices such as thyristors, even if the manufacturer runs the risk of losses. Further, resistance values immediately after transition to the nonsuperconducting state (off state) are small, and the cutoff characteristics are not satisfactory. These have been indicated as problems.

The authors, et al., thought to facilitate the transition between superconductivity and nonsuperconductivity by irradiating light to superconductors, and carried out basic experiments. As a result, we have found that irradiation of light causes voltage-current characteristics to change; the results are reported below.

Results and Discussion

A specimen, $Bi_2Sr_2CaCu_2O_3$ (10 percent Ag added), was prepared by the FZ process. The specimen was rectangular in shape, and its size was 0.9~2.0 mm x 0.5 mm x 20 mm. Using indium, the specimen was soldered directly onto a copper block that had high heat capacity and heat conductivity. Its V-I characteristics were measured in liquid nitrogen using the four-probe method. An electric current was applied by the linear rising method of 1~5 s in width. Then the V-I characteristics were compared between the case where visible rays were

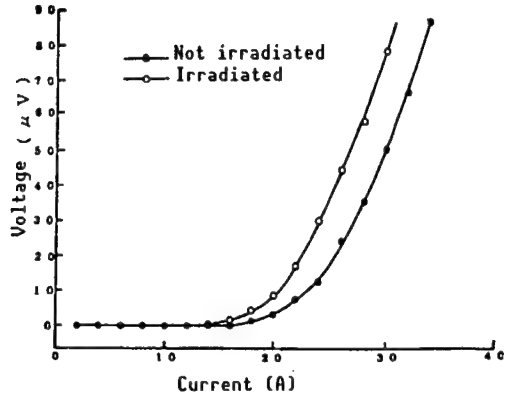

Figure 1. Effect of Irradiation on V-I Characteristics

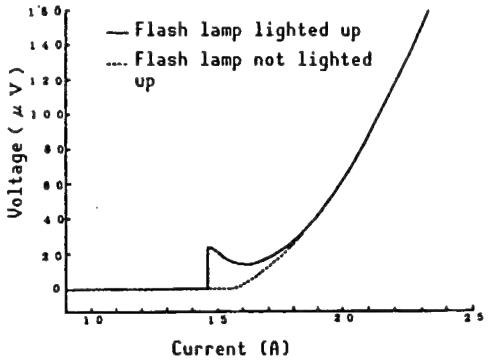

Figure 2. Effect of Irradiation by Flash Lamps 18 A/s (1 A/56 ms) Linear Rising Current

irradiated to the specimen and the case where no visible rays were irradiated. A slide projector and a photography flash lamp were used as light sources.

V-I characteristics were compared under different environments, that is, under light irradiation and in the dark (Figure 1). The figure shows that the critical current density lowers during the irradiation of light unlike being in the dark, and that the voltage rising rate increases. This trend becomes conspicuous as the width of the specimen and the light receiving area increase.

When we were measuring the V-I characteristics of the specimen, we suddenly started irradiating light to it. From this point on, the voltage rising ratio increased. Figure 2 shows the V-I characteristics of the specimen when light pulse was irradiated using a flash lamp.

The figure shows that a voltage was generated by light pulse, although the current value lowered the critical current value, and that the voltage generated attenuated and disappeared in a short period of time.

The following can be thought of as the effects of light on superconductors.

(1) The irradiation of light with an energy that exceeds the superconducting energy gap causes superconducting electron pairs to be broken.

(2) The irradiation of light causes flux pinned at pinning centers to easily escape.

(3) Light is absorbed by the lattice, and the specimen temperature thereby rises.

These effects serve to facilitate the transition of the specimen from the superconducting to the nonsuperconducting state. As shown in Figure 2, however, the specimen responded to pulse light. In addition, the amount of radiation heat calculated roughly, with consideration given to the light

source efficiency and the solid angle of the specimen, is exceptionally smaller than Joule heat generated by the contact resistance. It is thought, therefore, that items (1) and (2) above have large effects on V-I characteristics, compared with item (3) "rise in temperature."

The detailed mechanism requires future study. The use of effects of light, however, may improve the superconducting switch operation speed, and thereby lead to development of switching devices that can be operated at speeds faster than the conventional superconducting switches using heat and magnetic field. It is also expected that electric resistance rises in the nonsuperconducting state immediately after transition, and that cutoff characteristics are improved.

Conclusion

We found that the irradiation of visible light to Bi-based oxide superconductors causes the critical current density to lower and that transition to a nonsuperconducting state can be facilitated. As a result, we have been able to indicate the possibility that light triggered superconducting switching devices may be developed using the said phenomenon.

We would like to thank the Fine Ceramics Center Functional Material Department that offered us specimens.

References

1. Kubo, Y., et al., JJAP, Vol 28 No 11, 1989, pp L1936-1938.

2. Shimizu, N., et al., Ibid., pp L1955-1958.

3. Yoshida, Shimizu, et al., Electrical-Related Society, Tokai Branch Association Meeting, 1990.

Larger QMG Material (I)

916C0018 Tokyo TEION KOGAKU CHODENDO GAKKAI YOKOSHU in Japanese 23-25 Nov 90 p 122

[Article by Mitsuru Morita, Seiki Takebayashi, Keiichi Kimura, Masamoto Tanaka, Katsuyoshi Miyamoto, and Kiyoshi Sawano, No. 1 Technical Research Laboratory, Nippon Steel Corporation]

[Text] **1. Introduction**

Y-based superconducting materials prepared by the quench and melt growth (QMG) process have a high critical current density (J_c) at liquid nitrogen temperature; their characteristics are not amenable to practical use environments. We have reported on these at the '88 Spring Meeting,[1] for example. This report describes the increase in size of superconducting materials prepared by the QMG process that use differences in the growth temperature of the superconducting phase crystals of systems, including various rare-earth elements. In addition, we report on the characteristics of bulk materials (thus prepared) as magnets.

2. Larger Size

(1) Fabrication of Larger Size Antecedent Part by Lap Quenching

The 123 powder containing excessive 211 was melted at about 1,450°C, and quenched using two copper plates. Thus, a plate of about 2 mm in thickness was fabricated. Next, a melt was put on this plate, and quenched using a copper plate. Repetition of these operations made it possible to fabricate fine, thick antecedent parts. Figure 1 shows the structure of a cross section of the quenched materials that overlapped with each other in layers.

(2) Change in 123 Formation Temperature Due to Replacement of $REBa_2Cu_3O_{7-x}$ With Rare-Earth Elements

The temperature (T_n) at which 123 crystals are formed by the QMG process depends on ion radius, and greatly changes by replacing the Y site with other rare-earth elements. Individual systems showed the following 123 crystal formation temperatures.

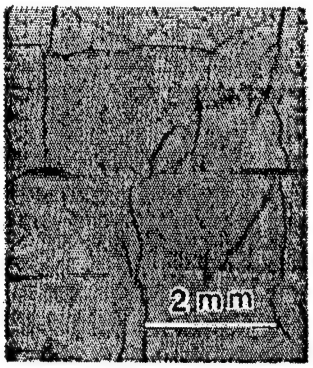

Figure 1. Structure of Lap-Quenched Antecedent Part

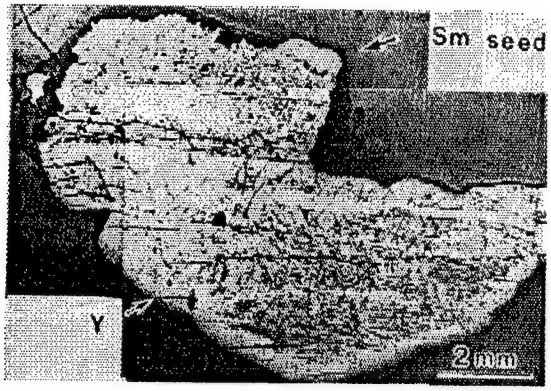

Figure 2. Structure of Y-Based Specimen Obtained Using Sm-Based QMG Material as Seed Crystal

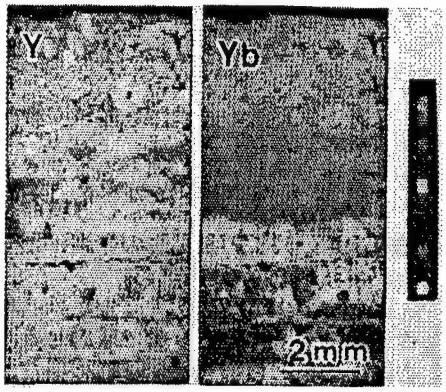

Figure 3. Distribution of Elements of Y-Yb-Based Specimen Unidirectionally Grown by Providing a Composition Gradient

- Sm system: about 1,060°C
- Ho system: about 1,000°C
- Yb system: about 900°C

It was also found that a mixture of several types of rare-earth elements causes its T_n to become nearly a mol average of the T_n of each rare-earth element.

1) Crystal Orientation Control of High T_n Composition Using Seed Crystals

Seed crystals were cut from an Sm-based QMG material, and its cleaved surface was made to come into contact with the antecedent part (placed in a half melted state) of a Y-based QMG material. Thus, Y-based QMG crystals with the same orientation were grown, and a specimen, as shown in Figure 2 was obtained. The figure shows the structure of this specimen.

2) Unidirectional Growth of Crystals at Uniform Temperature Using Rare-Earth Element Composition Gradient

To control nucleation from crystals other than seed crystals, crystals were unidirectionally grown using a rare-earth composition gradient. Changing the ratio of Y to Yb, crystals were unidirectionally grown at a uniform temperature by using Sm-based seed crystals for the lap quenched antecedent part, and a specimen was obtained. Figure 3 shows the distribution of elements of the specimen.

These processes have made it possible to prepare large mock single crystal-shaped bulks.

3. Flux Trap

Using the above processes, a bulk whose size was greatly increased was cooled to the liquid nitrogen temperature in a magnetic field, and magnetic flux was lapped in the superconductor. As a result, a maximum magnetic flux density of 3,200 G was observed on the surface of a specimen of 34 mm in diameter and 13 mm in thickness.

References

1. Morita, et al., NSMF NEWS, No 10, 1988, p 15.

Larger QMG Material (II)

916C0018 Tokyo TEION KOGAKU CHODENDO GAKKAI YOKOSHU in Japanese 23-25 Nov 90 p 123

[Article by Katsuyoshi Miyamoto, Kiyoshi Sawano, Mitsuru Morita, Masamoto Tanaka, Keiichi Kimura, and Seiki Takebayashi, No. 1 Technical Research Laboratory, Nippon Steel Corporation]

[Text] **1. Introduction**

The improvement of the quench and melt growth (QMG) process has made it possible to prepare larger Y-based oxide superconductor bulks. Larger bulks can be cited to be put into practical use as superconducting magnets using magnetic characteristics and as contactless bearings using magnetic repulsive force, for example. To apply magnetic repulsive force and adsorption force, it is important to qualitatively grasp these forces. Therefore, we studied factors that contribute to these characteristics, together with the method of evaluating magnetic repulsive force and adsorption force.

2. Evaluation

Specimens ranging from 20~50 mmϕ and 5~30 mmt, prepared by improving the QMG process, were used for measurements. Figure 1 shows an outline of the measuring equipment.

A permanent magnet (Sm-Co, 50 mmϕ, 10 mmt) of 2,800 G was installed at the end of the load cell, using a tensile tester, and the specimen was put in a vessel filled with liquid nitrogen. The specimen was processed into the same or smaller size as that of the permanent magnet. Thus, measurements were carried out on the assumption that a magnetic field is uniformly applied to the specimen. At the initial stage of measurement, a sufficient distance (50 mm) was provided between the permanent magnet and the specimen. Thus, repulsive force produced within the distance from the position where repulsive force has not yet occurred to the position where the permanent magnet comes into contact with the specimen, was measured continuously. Further, adsorption force produced when the permanent magnet was pulled apart from the contact state and resulting from the state in which magnetic flux is trapped in the specimen, by field cooling under a magnetic field, was measured continuously to evaluate magnetization characteristics.

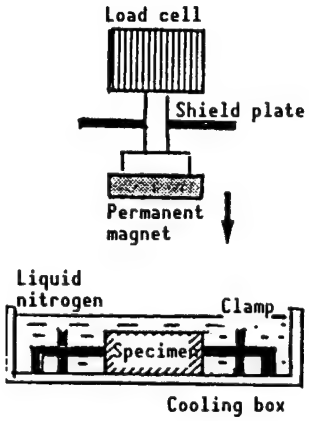

Figure 1. Outline of Measuring Equipment

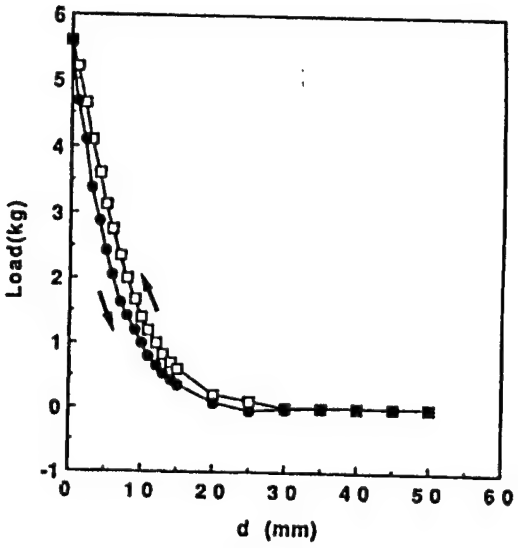

Figure 2. Magnetic Repulsive Force of QMG Material

3. Results and Discussion

Figure 2 shows a typical example of the results of measurements using the above method.

With every specimen, when the magnet was brought closer to the specimen, to a distance of about 10 mm, the repulsive force rapidly increased. Further, when the magnet came into contact with the specimen, the adsorption force due to magnetic flux trapped in the specimen showed its maximum value in the region where the distance between the magnet and specimen becomes less than about 10 mm and the effect of repulsive force thereby decreases. Repulsive force ranged from 2.4~5.6 kg between specimens having the same size. This large difference in repulsive force was caused mainly by different crystal particle sizes, because specimens were made of crystal particles of about 10 mm and of 20~30 mm. There was no large change in the microstructure between specimens studied for this research. The effect of oxygen also appeared, and the repetition of oxygen annealing served to improve repulsive force.

Trial Manufacture of Y-Based Large-Size Thin Film Coil

916C0018 Tokyo TEION KOGAKU CHODENDO GAKKAI YOKOSHU in Japanese 23-25 Nov 90 p 124

[Article by Noriharu Tamada, Isao Maeda, and Hiroshi Yamamoto, Electric Research Institute and Engineering Department of Nihon University]

[Text] **1. Introduction**

It is known that oxide superconductors react with Al and Si by heat treatment. Therefore, we attempted to manufacture large-size Y-based superconducting thin film coils, into which patterning using Al was introduced; using the RF magnetron sputtering process enabled uniform thin films to be obtained over a wide area. We also studied the manufacturing process.

2. Experiment

A pattern using Al was prepared on a substrate before film formation or on an already formed thin film. Then, a thin film coil was prepared from superconducting thin films separated through the annealing process from the portion that reacted with the Al. The film formation conditions were:

- Substrate for film formation: MgO (100)
- RF power: 300 W (RF power density: 0.93 W/cm^2)
- Sputter gas: Ar = 8 mTorr
- Film formation time: 1 hour

The superconducting characteristics of the thin films formed were optimized by annealing. Then, under the above conditions, thin film coils were manufactured by annealing. Crystallinity and composition were measured by X-ray diffraction and inductively coupled plasma (ICP), the surface was observed by scanning electron microscope (SEM), and the critical temperature (T_c) was measured by the four-probe method.

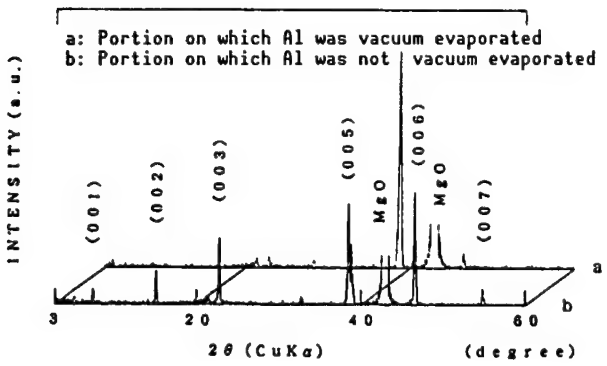

Figure 1. X-Ray Diffraction Diagram

Figure 2. SEM Image

3. Results and Discussion

With respect to the film thickness distribution based on the substrate position as deposited, almost constant films were obtained over the large-size substrate of 60 mmϕ. Composition analysis by ICP has also confirmed that the film thickness was uniformly distributed. The substrate was not particularly heated and, therefore, required crystallization processing at high temperatures. Uniform heat treatment, however, made it possible to easily obtain large-size thin films. Next, Al was vacuum evaporated on a part of the thin films formed, and the films were annealed at 940°C in air. An X-ray diagram of the specimen thus prepared is shown in Figure 1.

Figure 2 shows an SEM image of the surface of the film based on the presence or otherwise of Al vacuum-evaporated film. According to this figure, it can be observed that a (123) phase with a good c-axis orientation grew at the portions on which Al was not vacuum evaporated. However, at the portions on which Al was vacuum evaporated, growth of a superconducting phase was controlled; the appearance of a new phase that seems to partially contain Al can be observed. We intend to report on the details at the meeting.

Application of Oxide Superconductor to Magnet

916C0018 Tokyo TEION KOGAKU CHODENDO GAKKAI YOKOSHU in Japanese 23-25 Nov 90 p 125

[Article by Masano Mimura, Naoki Uno, and Yasuzo Tanaka, Yokohama Research Laboratory; and Katsuo Oishi, Superconducting Products Department, New Function Division, Furukawa Electric Co., Ltd.]

[Text] **1. Introduction**

Various studies have been carried out concerning application for oxide superconductors at the liquid nitrogen temperature. As an application to magnets, however, wires with sufficient J_c characteristics have not yet been obtained because of weak links, weak pinning, and flux creep, for example. On the other hand, oxide superconductors possess an upper critical magnetic field that extends over several hundred tesla at 4.2 K. They, therefore, are receiving much attention as materials for use in high magnetic fields. In this research, we studied the application of Bi-based (2212) phase Ag composite materials to magnets used in high magnetic fields.

2. Experiment

An Ag pipe was filled with Bi-based (2212) phase powder, then processed and heat treated. Thus, superconducting tape wires ranging from 0.1~0.2 mm in thickness and 3~4 mm in width were prepared. These wires were evaluated in regard to their characteristics and were processed into coils.

Evaluation of Wires

• J_c-B characteristics (4.2 K)

Figure 1 shows the high magnetic field characteristics of J_c at 4.2 K. With an increase in the c-axis orientation rate (F) of crystals, J_c increased. At 30 T, $J_c = 2.1 \times 10^5 A/cm^2$ was obtained. Thus, Bi-based wires have sufficient J_c characteristics for application to magnets used in high magnetic fields.

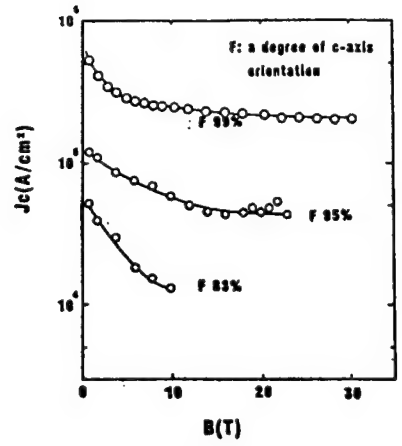

Figure 1. High Magnetic Field Characteristics of J_c at 4.2 K

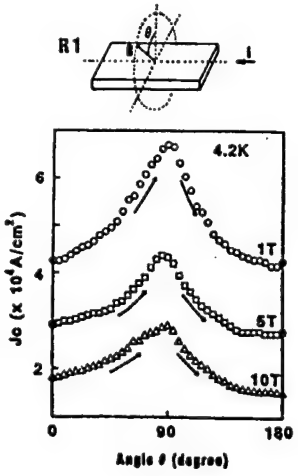

Figure 2. Anisotropy of J_c Due to Applied Magnetic Field Direction

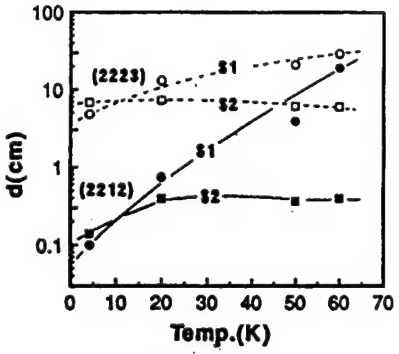

Figure 3. Thickness of Superconductor Satisfying Adiabatic Stabilization (S1) and Dynamic Stabilization (S2)

- **J_c-θ characteristics (anisotropy of J_c due to applied magnetic field direction)**

Figure 2 shows the anisotropy of J_c that results from changes in the size of applied magnetic fields. The figure shows that there is little change in anisotropy due to magnetic field and that J_c (θ = 0°)/J_c (θ = 90°) is about 0.6. From these results, it can be thought that this anisotropy does not pose any large problems in the application of wires to magnets at 4.2 K.

- **Study for stabilization**

Figure 3 shows changes in the thickness of superconductors according to temperatures, which satisfies both adiabatic and dynamic stabilization. The figure shows that even if the thickness of the superconductor is about 0.1 cm at 4.2 K, this can fully satisfy the requirements for adiabatic and dynamic stabilization. It does not appear, therefore, that the conventional adiabatic and dynamic stabilization obtained by fabricating multicore wires is necessary for Bi-based superconductors.

Fabrication of Coil

On the basis of the above results of experiments, we fabricated pancake coils for trial. The tape material used was 0.2 mm in thickness and 4 mm in width. The coil fabricated was a pancake shape, and was 20 ϕ in inside diameter and 34 ϕ in outside diameter, and had 22 turns. The wind-and-react (W&R) process was employed. Using oxide superconducting magnets thus obtained, we were able to produce maximum magnetic fields of 0.12 T and 0.11 T, at 4.2 K, in outer layer magnets, 0 T and 1 T, respectively.

3. Conclusion

We fabricated Bi-based Ag composite wires, and evaluated their superconducting characteristics at 4.2 K. As a result, we have been able to clarify that Bi-based Ag composite wires can be fully applied to magnets used in high magnetic fields. On the basis of these results, we fabricated small coils for trial, and were able to produce a maximum magnetic field of 0.11 T, at 4.2 K, in an outer layer magnet, 1 T.

The evaluation of wires at 4.2 K was carried out with the Kazumasa Togano's group of National Research Institute of Metals, Science and Technology Agency, on a joint research basis. Further, we used the superconductor development facilities of the Metal Material Research Laboratory, Tohoku University, to measure high magnetic fields up to 30 T.

Elementary Technology To Fabricate Coils Using Bi-Based Oxide Superconductors

916C0018 Tokyo TEION KOGAKU CHODENDO GAKKAI YOKOSHU in Japanese 23-25 Nov 90 p 126

[Article by Kazutetsu Naohara, Masaharu Yasuhara, and Mamoru Ishihara, Hiratsuka Research Laboratory, Sumitomo Heavy Industries, Ltd.]

[Text] **1. Introduction**

The use of various processes has served to greatly improve the critical current density J_c of Bi-based oxide superconductors. This is necessitating the development of elementary technology to fabricate superconducting coils. In particular, it is necessary to select insulation materials suited to the heat treatment conditions in fabricating coils by the wind-and-react (W&R) process. Therefore, we fabricated pancake coils for trial, using Ag-sheathed wires insulated with ceramic fiber, and studied whether superconducting coils can be fabricated.

2. Experiment

An Ag pipe was filled with calcined powder prepared by the general solid phase reaction process, then the powder was drawn and rolled. Thus, Ag-sheathed tapes ranging from 1~1.5 m in length and 0.2~0.3 mm in thickness were prepared. These tapes were insulated with ceramic fiber, and wound on an MgO ceramic cylinder (25 ϕ) to prepare pancake coils. These pancake coils were heat treated at 800~840°C for 100 hours, underwent cold isostatic pressing (CIP) treatment, and were heat treated again. The critical current was measured in liquid nitrogen by the general four-probe method.

3. Results and Discussion

To investigate the effect on superconducting characteristics from using ceramic fiber, straight short wires were insulated with ceramic fiber and heat treated. Thus, the critical current of the heat treated wires was measured. As a result, a critical current of 90 percent of the wires not having been coated with ceramic fiber was obtained. It has been confirmed, therefore, that ceramic fiber can be used as insulating materials.

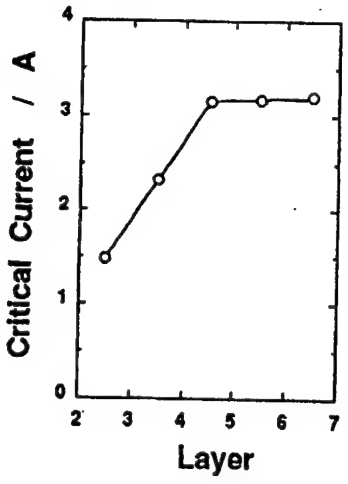

Figure 1. I_c Per Layer

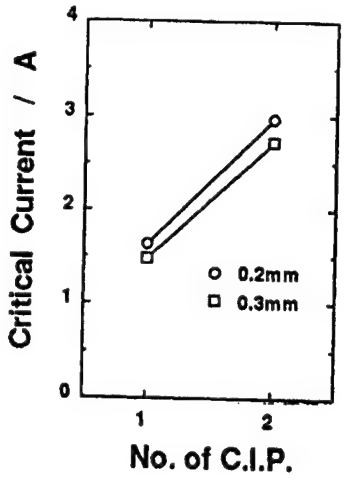

Figure 2. Effect of CIP Treatment on I_c

Figure 1 shows the critical current per layer when Ag-sheathed tapes were wound in seven layers in the form of a pancake coil. The critical current lowered from the outer layers toward the inner layers. However, no changes in the critical current were observed on the fourth through the seventh layers. This is estimated to result from the inner part of the coil having a large curvature. Further, the critical current of the entire coil corresponds nearly to that of the innermost layer.

Figure 2 shows the effect of the number of CIP treatments on the critical current of pancake coils made of conductors, in which wires of 0.2 mm and 0.3 mm in thickness, respectively, are insulated using ceramic fiber. The figure shows that as the number of CIP treatments increases, the critical current increases. It has been confirmed, therefore, that CIP treatments prove effective as an intermediate pressurization process for pancake coils. Further, the wire of 0.2 mm in thickness was compared with that of 0.3 mm in thickness. As a result, the former showed a critical current higher than that of the latter. In view of the critical current density, it is thought that fabrication of coils using wires of 0.2 mm in thickness is more advantageous.

Fabrication of Coils Using Bi-Based Oxide Superconducting Tape

916C0018 Tokyo TEION KOGAKU CHODENDO GAKKAI YOKOSHU in Japanese 23-25 Nov 90 p 127

[Article by Yuu Kitamura, Takayo Hasegawa, and Kouki Kobayashi, Showa Electric Wire & Cable Co., Ltd.; and Hiroyasu Hagiwara, Akatsuki Murase, and Kazuo Yamamoto, Toshiba Corporation]

[Text] **1. Introduction**

With respect to Bi-based superconducting tapes prepared by the Ag-sheath process, research is being conducted to develop longer tapes with higher J_c and I_c, and thereby to apply these tapes to coils. For this research, we fabricated solenoid coils by the wire-and-react (W&R) process, using Bi-based Ag-sheathed tapes, and studied their electrical characteristics.

2. Experiment

An Ag pipe was filled with calcined powder with Bi(Pb) 2223 composition, then drawn and rolled. Thus, a tape of 0.15 mm in thickness and about 3 m in length was prepared. This tape was cut per meter, and one-layered or two-layered tapes were wound on a ceramic pipe 34 mm in diameter in the form of a solenoid. In this way, coils were fabricated by the W&R process. The electrical characteristics of these coils were measured at 77 K and 4.2 K (I_c was defined at 0.1 μV/cm). The condition of the core was investigated by X-ray diffraction and scanning electron microscope (SEM).

3. Results

To prepare coils, lengthy tapes are calcined, and their characteristics are thought to be lower compared with those of short tapes. Table 1 presents the electrical characteristics of a short tape and coils prepared by the same process.

Processing lengthy tapes into coils caused their I_c to lower, but I_c of about 90 percent of that of the short tape was obtained.

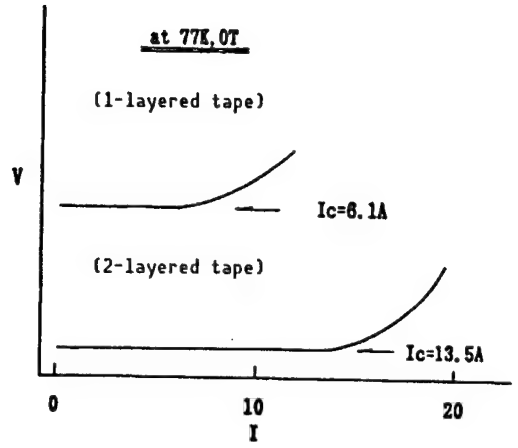

Figure 1. I–V Characteristics of Solenoid Coil Fabricated

Table 1. Changes in I_c Caused by Fabricating Lengthy Tapes

	Short tape	Coil	
Length	3	30	100
Number of turns	—	3	10
I_c(A)	7.1	6.5	6.1
J_c(A/cm^2)	7100	6500	6100

We measured J_c of coils (prepared using a tape 1 m long) at 77 K and 0 T. The results are shown in Figure 1.

The one-layered tape coil showed an I_c of 6.1 A (J_c = 6.1 x 10^3A/cm^2), whereas the two-layered tape coil showed 13.5 A (J_c = 6.3 x 10^3A/cm^2). Thus, I_c was improved about two times, although J_c was approximately the same. This shows that I_c of coils can be improved by winding tapes in multilayers.

We are further studying the fabrication of coils using multilayered longer tapes, and intend to report on the results of the study at the meeting.

Manufacture of Coils Using Bi-Based Ag-Sheathed Tapes

916C0018 Tokyo TEION KOGAKU CHODENDO GAKKAI YOKOSHU in Japanese 23-25 Nov 90 p 128

[Article by Toshie Takeuchi, Shoichi Yokoyama, Kenji Shimohata, Shiro Nakamura, Central Research Laboratory; and Shoji Miyashita and Fumio Fujiwara, Material Research Laboratory, Mitsubishi Electric Corporation]

[Text] **Introduction**

We are currently conducting research on the improvement of J_c of Bi-based Ag-sheathed tape wires and on applications for these materials. In this research, we studied the fabrication of coils using Bi-based Ag-sheathed tapes by carrying out stabilization and magnetic field analysis.

Experiment

A Bi-based Ag-sheathed tape with 2212 phase (matrix ratio: 3) was used for experiments. The size of the tape was 3 mm in width and 0.2 mm in thickness. The critical current density $J_{c_{sc}}$ (measured by the four-probe method) of the superconductor was $2.2 \times 10^4 A/cm^2$ at 4.2 K and B = 1 T. Figure 1 shows the magnetic field dependence of $J_{c_{sc}}$ of this tape.

Results and Discussion

The complete stability of coils is rated based on stabilization coefficients, i.e., $\alpha = G/Q$,[1] that are obtained by the heating value G and cooling value Q of conductors or entire coils. If the stabilization coefficient (α) of a conductor is smaller than 1, that is, $\alpha < 1$, the conductor is thought to be a completely stabilized conductor. The stabilization coefficient at $J_{c_{sc}}$ (at 4.2 K, 1 T) of a Bi-based Ag-sheathed tape cooled in liquid He is $\alpha = 1.69 \times 10^{-4}$ and, therefore, this tape is a completely stabilized conductor. In the case of a 150-layered pancake wound solenoid coil, cooled in liquid He, the cooling perimeter amounts to about 1/150, but the stabilization coefficient is $\alpha = 2.53 \times 10^{-2}$, showing that this coil is a completely stabilized conductor.

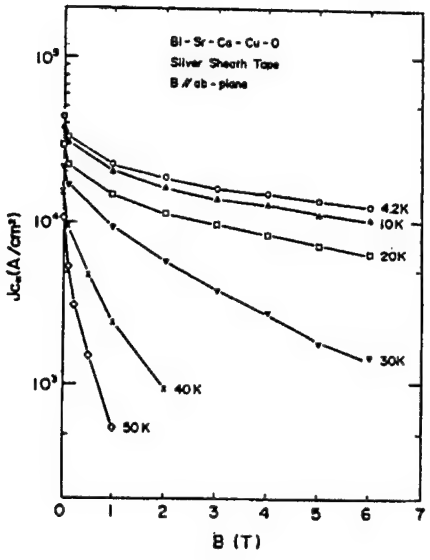

Figure 1. $J_{c_{sc}}$–B Characteristics of Bi–Based Tape

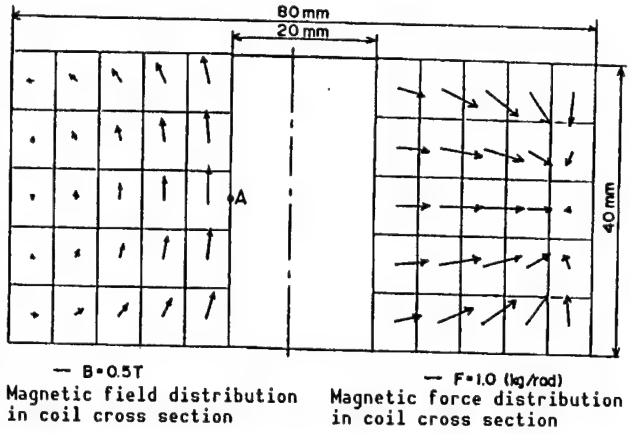

Figure 2. Magnetic Field Analysis of Coil Using Bi Tape

We conducted magnetic field analysis of a 150–layered coil, and designed a 1 T magnet. Figure 2 shows a distribution of magnetic fields (in the cross section of the coil) and magnetic force.

The designed coil was 20 mm ϕ in inside diameter, 80 mm ϕ in outside diameter, and 40 mm in height. When the mean current density in the coil cross section was $4.2 \times 10^3 A/cm^2$, the central magnetic field B_0 became 1.0 T. B_{max} was 1.2 T and located at point A. From the mean current density in the cross section, the current density of the superconductor became $1.7 \times 10^4 A/cm^2$. This value is smaller than that where consideration is given to the lowering of $J_{c_{sc}}$ due to the angle dependence[2] of magnetic field at the coil peripheral portion. The fabrication of coils using Bi–based Ag–sheathed tapes, therefore, is thought to be able to be achieved under the above conditions.

References

1. Nishi, M., CRYOGENICS ENGINEERING, Vol 24 No 4, 1989.

2. Shimohata, et al., 1990 Autumn Cryogenics Engineering Preliminary Draft B–1–7.

Fabrication, Evaluation of Ag-Sheathed Bi-Based Superconducting Coil

916C0018 Tokyo TEION KOGAKU CHODENDO GAKKAI YOKOSHU in Japanese 23-25 Nov 90 p 129

[Article by Keisuke Yamamoto, Junichi Kai, and Makoto Hiraoka, Central Research Laboratory, Mitsubishi Cable Industries, Ltd.]

[Text] **1. Introduction**

For fabricating lengthy, multicore wires using oxide superconductors, processing them into coils, and stabilizing them, silver-sheathed superconducting wires fabricated by the powder-in-tube process have many advantages compared with wires fabricated by other processes. Paying attention to this point, we are conducting research and development of Ag-sheathed $Bi_2Sr_2Ca_2Cu_3O_y$ superconducting tape for application to wires. J_c of this type of single-core tape at 77 K has recently been considerably improved. We have also been able to stably prepare tapes with a J_c of about 2 x $10^4 A/cm^2$ (B = 0). Therefore, to fabricate lengthy wires and process them into coils, we prepared small coils, evaluated their characteristics, and report on the results below.

2. Experiment

The charge composition ratio of the oxide superconductor was established to be Bi:Ph:Sr:Ca:Cu = 0.9:0.2:1.0:1.1:1.5. Then, an Ag-sheathed tape of 0.2 mm in thickness, 2.6 mm in width, and about 10 m in length was prepared by the general powder-in-tube process. This tape was cut into pieces that ranged from 0.6~1.2 m in length. These cut pieces were wound on a ceramic reel of 30 mm in outside diameter, and sintered at 830°C for 160 hours in air. Further, of the sintered pieces, some pieces were unwound, rolled, and again processed into coils. Thus, coils repeatedly sintered at 830°C for 40 hours, and coils sintered in the same manner after pressing were fabricated. The fabricated coils were evaluated by measuring their I_c in liquid nitrogen by the dc four-probe method. I_c was defined to be 1 $\mu V/cm$, and J_c was calculated based on the sectional area obtained by removing the Ag-sheathed portion from the entire tape sectional area.

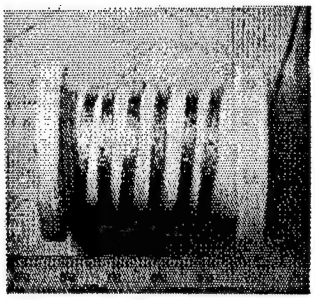

Figure 1. Superconducting Coil

3. Results

Table 1 presents the characteristics of the coils prepared by the three different processes. Further, Figure 1 shows a photograph of the appearance of a coil intermediately pressed. The table reveals that J_c extending over the entire length (the longest distance between voltage terminals) of a coil becomes higher in the order of only sintered coil (J_c = 820 A/cm^2), intermediately rolled coil (J_c = 1,900 A/cm^2), and intermediately pressed coil (J_c = 6,300 A/cm^2). It can be seen that intermediate pressing greatly improves J_c. This shows that measures for improving J_c by intermediate pressing (reported many times through tests on short tapes)[1] can be applied to lengthy tapes. Every coil, however, shows uniformity in J_c in the longitudinal direction, which, therefore, must be studied in the future.

Table 1. Characteristics of Coils (77 K) Prepared by Various Processes

Coil number	S-1	SRS-1	SPS-1
Treatment conditions	Only sintering	Intermediate rolling	Intermediate press
I Max. (cm)	118	78	6
I_c (A)	1.9	3.2	10.1
J_c (A/cm^2)	820	1,900	6,300
J_c Max.	1,100	4,000	8,100
J_c Min.	610	1,000	5,700

Note: $J_{c_{max}}$ and $J_{c_{min}}$ show maximum and minimum J_c values (A/cm^2), respectively, per turn (1 = 9.8 cm) of coil.

References

1. For example, Osamura, K., et al., SUPERCOND. SCI. TECHNOL., Vol 3, 1990, p 143.

Development of Superconducting Current Limiting Relay

916C0018 Tokyo TEION KOGAKU CHODENDO GAKKAI YOKOSHU in Japanese 23-25 Nov 90 p 156

[Article by Taiso Ito, Eriko Yoneda, Kazuyuki Tsurunaga, and Yoshiyuki Sugiyama, Toshiba Corporation; and Chikushi Hara, Kiyoshi Okaniwa, and Takahiko Yamamoto, Tokyo Electric Power Co., Inc., Technical Research Laboratory]

[Text] **1. Introduction**

There is a growing desire for development of superior current limiting relays that do not involve loss during stationary operation and that can easily obtain actuation impedance. To verify whether superconducting current limiting relays can comply with such needs, we have developed 400-V, 100-A class superconducting current-limiting relays, subsequent to the 100-V, 50-A class superconducting current-limiting relays described in our previous report. The structure of the new relays has been improved so that they can be used immediately after actuation.

2. Principle of Operation

Unlike the 100-V, 50-A class current-limiting relays, the newly developed 400-V, 100-A class superconducting current-limiting relay is of a construction in which two coils, connected in series, are wound in such a way that they become noninductive, thus comprising a trigger coil (Figure 1).

These coils are wound using superconducting wires. Therefore, as far as they are placed in a superconducting state, their impedance as observed from the outside amounts to zero. This trigger coil is connected in parallel with a superconducting reactor (current-limiting coil), thereby comprising a current-limiting relay. When accidents occur, the trigger coil is quenched, and the current-limiting coil controls the accident current by its inductance, with the superconducting state of the current-limiting relay maintained. This current-limiting relay also was an auxiliary trigger coil (trigger coil 2), in addition to the main trigger coil 1 (Figure 1). Therefore, trigger coil 1, when quenched by accident current, is changed over to trigger coil 2 by operating the switch, and the current-limiting relay can be restored to the superconducting state.

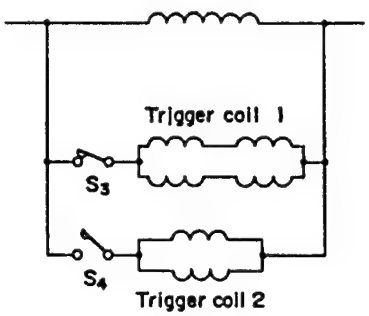

Figure 1. Structure of 400-V, 100-A class Superconducting current-limiting relay

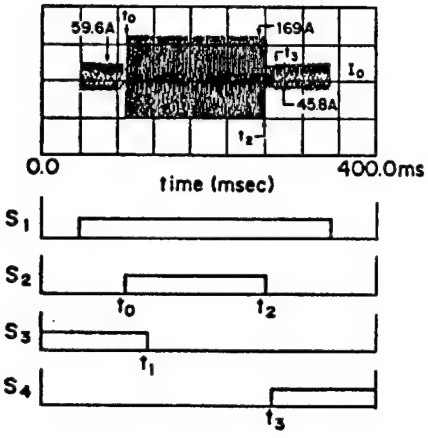

Figure 2. Test Circuit

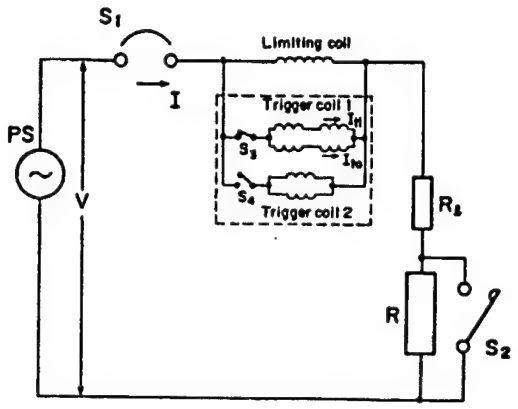

Figure 3. Operating Characteristics

3. Results

This current-limiting relay was put in the circuit shown in Figure 2, and operation verification tests were conducted. A resistance of 10 Ω was inserted by applying a load R.When switch S_2, located in parallel with this load R, was close,d a short-circuit current flowed in the current-limiting relay. As shown in Figure 3, 420 V was applied before time t_0, and a current of 42 A was flowing in the circuit. When S_2 was closed at time t_0, and the current flowing in the circuit reached 100 A,trigger coil 1 was quenched, and the current-limiting relay was operated. In this case, a current of 169 A, which is determined by the current-limiting coil impedance, flowed in the current-limiting coil. Thus, it has been confirmed that the use of the current-limiting relay makes it possible to control short-circuit currents to any optional value, for example, 169 A in this experiment. Further, at time t_2, S_2 was opened, and the short-circuit state was canceled. At time t_3, trigger coil 2 was connected, and the same current as that before time t_0 flowed. It has also been confirmed, therefore, that this current-limiting relay can be momentarily reset to the original superconducting state.

4. Conclusion

We developed a 400-V, 100-A class superconducting current-limiting relay provided with an auxiliary trigger coil for momentary reset, and confirmed that this relay can be operated as per the design. We intend to develop relays with a larger capacity in the future.

Tube Process Nb_3Sn Wire Using Alumina Distributed Reinforced Copper Matrix (Part I)

916C0018 Tokyo TEION KOGAKU CHODENDO GAKKAI YOKOSHU in Japanese 23-25 Nov 90 p 177

[Article by Noriyuki Shiga, Nobuo Aoki, and Masamitsu Ichihara, Showa Electric Wire & Cable Co., Ltd.; and Shigeo Nakayama, Akatsuki Murase, and Keizo Shimamura, Toshiba General Research Institute]

[Text] **1. Introduction**

Appearance of large superconducting magnets requires development of Nb_3Sn superconducting wires that are strong enough to withstand high electromagnetic force. It is desirable, therefore, that materials (with high conductivity) capable of maintaining high strength, even if they are heat treated at high temperatures, be used for the matrix. For this research, we used alumina dispersed copper for part of the matrix in the case of Nb_3Sn wires (prepared by the tube process), and studied their processability and mechanical characteristics. Described below are the results of the research.

2. Properties of Alumina Dispersed Copper

The 0.2 percent yield strength of the alumina dispersed copper used for this research is 44 kg/mm^2, which is about six times that (7 kg/mm^2) of oxygen-free copper. Further, as shown in Figure 1, the hardening of this copper due to processing is small. Even if it is heat treated at the Nb_3Sn formation temperature of 700°C, the lowering of its strength is small. This copper, therefore, appears to be effective as matrix material for superconducting wires. Accordingly, we applied this copper to part of the Nb_3Sn superconducting wire matrix, fabricated Nb_3Sn wires for trial, and evaluated them.

3. Wires Fabricated for Trial

Two types of Nb_3Sn wires were fabricated by the tube process, for trial purposes. In other words, alumina dispersed copper (Cu-2Vol%Al_2O_3) and oxygen-free copper were respectively used for the outermost layer tube of each single wire. These single wires were processed in the form of a hexagon by cold drawing, bundled in large quantities, and inserted in an oxygen-free tube.

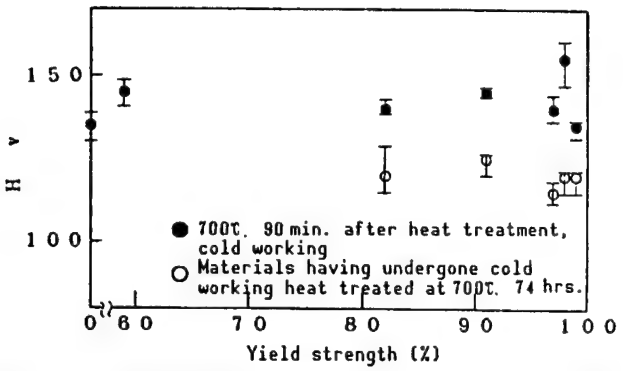

Figure 1. Hardening Property of Alumina Dispersed Copper Due to Processing

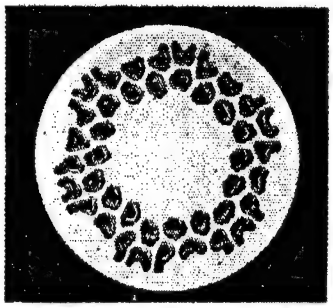

Figure 2. Cross Section of Wire Fabricated for Trial

This multi-wire was cold drawn, and its area was reduced until the outer diameter was ϕ1.04 mm. This wire was used as a specimen to measure mechanical and electric characteristics. Processability was also investigated until the outer diameter amounted to ϕ0.103 mm. Table 1 presents the specifications of the wires fabricated for trial, and Figure 2 shows a photograph on the cross section of the wire.

Table 1. Specifications of Wire Manufactured for Trial

	Al_2O_3 dispersed reinforced type	Oxygen-free copper (conventional) type
Wire diameter (mm)	1.04	1.04
Filament diameter (μm)	87.5	87.5
Number of filaments	42	42
Sn concentration (wt%)	50	50
Matrix ratio	Cu/Al_2O_3-Cu/non-Cu 1.74/0.63/1	Cu/non-Cu 2.37/1

4. Results

The oxygen-free copper wire showed good processability until its outer diameter was ϕ0.103 mm (filament diameter: 8.7 μm). It has been confirmed that the alumina dispersed reinforced wire can also be processed to ϕ0.103 mm. In other words, with respect to the alumina dispersed reinforced wire, the same processability as that of conventional oxygen-free wire was obtained.

Further, alumina dispersed copper was used for the Nb_3Sn superconducting wire prepared by the tube process, and the strength of the wire was thereby improved.

Tube Process Nb_3Sn Wire Using Alumina Dispersed Reinforced Copper Matrix (Part II)

916C0018 Tokyo TEION KOGAKU CHODENDO GAKKAI YOKOSHU in Japanese 23-25 Nov 90 p 178

[Article by Shigeo Nakayama, Akatsuki Murase, and Keizo Shimamura, Toshiba General Research Laboratory; and Noriyuki Shiga, Nobuo Aoki, and Masamitsu Ichihara, Showa Electric Wire & Cable Co., Ltd.]

[Text] **1. Introduction**

Alumina dispersed reinforced copper fabricated by the hydrogen reduction process, even if heat treated under Nb_3Sn formation heat treatment conditions (700°C or higher for 20~100 hours), is unlikely to be softened and has high conductivity,[1] in contrast with conventional copper alloys. Therefore, replacement of part of the Nb_3Sn wire copper matrix with alumina dispersed reinforced copper amy serve to improve the strength of this wire.

A few arrangement structures can be conceived for alumina dispersed reinforced copper in Nb_3Sn wires. In this research, we fabricated Nb_3Sn wires (for trial) whose entire copper matrix was replaced by alumina dispersed reinforced copper, and report on the results with emphasis on the electric conductivity.

2. Experiment

To compare an alumina dispersed reinforced copper matrix Nb_3Sn wire (tin concentration: 50 percent, number of Nb filaments: 42) with a conventional copper matrix Nb_3Sn wire (tin concentration: 50 percent, number of Nb filaments: 42), we measured I_c of these wires under the same heat treatment conditions.

3. Results

Figure 1 shows the J_c-magnetic field characteristics of the alumina dispersed reinforced copper matrix Nb_3Sn wire and the copper matrix Nb_3Sn wire. Both matrixes showed approximately the same J_c with respect to each magnetic field. There were no effects of alumina dispersed reinforced copper on the J_c values of matrix.

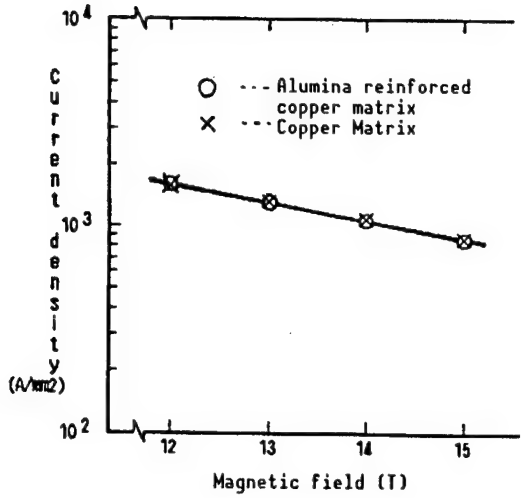

Figure 1. J_c–Magnetic Field

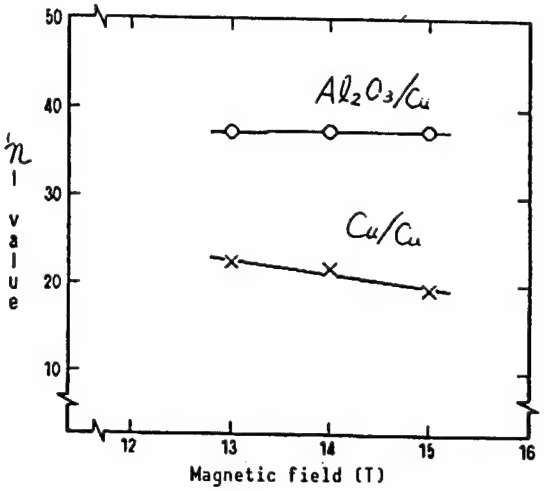

Figure 2. n Value–Magnetic Field

Figure 2 shows n values based on differences in matrix. The figure shows that n values of the alumina dispersed reinforced copper matrix were improved about twice those of the conventional copper matrix.

References

1. IEEE Tokyo Section, Denshi Tokyo, No. 28, 1989.

Toroidal SMES Principle-Demonstration System

916C0018 Tokyo TEION KOGAKU CHODENDO GAKKAI YOKOSHU in Japanese 23-25 Nov 90 p 219

[Article by Seiichiro Terai, Taiji Mizuguchi, and Kiyoshi Hasegawa, Kansai Electric Power Co., Inc.; Katsuyoshi Toyoda, Masaichi Fukada, and Naohiro Toki, Mitsubishi Electric Corp.; and Yoshishige Murakami, Engineering Department, Osaka University]

[Text] **1. Introduction**

As a toroidal-type superconducting magnetic energy storage (SMES) system, a voltage-type invertor plus chopper circuit system can be considered.[1] This system has many features, such as easy group control of many superconducting coils and easy parallel multiplex use of superconducting coils and converters. The authors, et al., planned test and research using a several MJ system (for trial) that incorporated this toroidal SMES system. We are currently conducting principle-demonstration tests on a system that uses two superconducting coils of 10 kJ class, prior to the manufacture of an actual model. This time, we conducted tests on the combination of superconducting coils with choppers, and report on the results below.

2. Principle-Demonstration Test

Figure 1 shows a principle-demonstration system. The system is composed of one voltage-type invertor, two choppers, and two superconducting coils, each of which is connected to each chopper. For this testing, we used a rectifier instead of the invertor. Table 1 presents the specifications of the system.

Figure 2 shows an example of energy transfer tests between superconducting coils. The first coil current (I_{L1}) was raised up to 196 A (5 T) in one second, and held for 0.5 second. Then, energy was transferred to the second coil in one second. The second coil current (I_{L2}) increased up to a maximum of 155 A, and slowly attenuated due to the circuit resistance.

In a series of tests conducted this time, input and output of triangle/sine waves into and from superconducting coils using choppers were repeatedly conducted at high speed. As a result, the fundamental operation characteristics of superconducting coil excitation by choppers were confirmed.

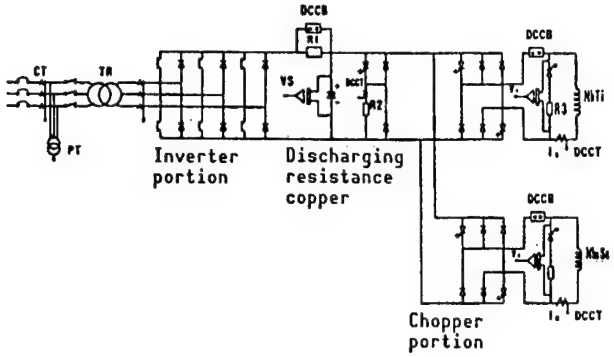

Figure 1. Principle-Demonstration System

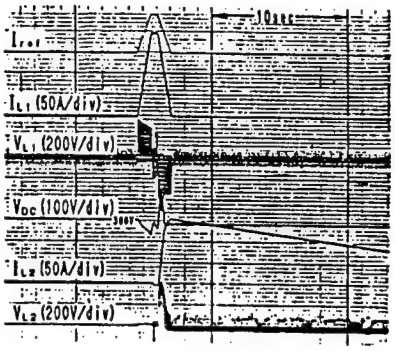

Figure 2. Energy Transfer Test Between Superconducting Coils

Table 1. Specifications of Principle-Demonstration System

Converter system	Voltage type invertor + chopper			
Invertor portion rating	20 kVA	22 V	52 A	1 unit
Chopper portion rating	60 kVA	400 V	150 A	2 units
	Switching frequency			300 Hz

	No. 1 coil	No. 2 coil
Superconducting coil system	NbTi immersed cooling	Nb_3Sn immersed cooling
Coil dimensions (mm) (inner diameter x outer diameter x height)	35 x 130 x 72	35 x 130 x 74
Rated current (A)	196	170
Maximum empirical magnetic field (T)	5	5
Stored energy (kJ)	17.3	18.1
Coil mean current density (A/mm^2)	86	85

We intend to conduct demonstration tests on the entire system, in combination with an invertor.

References

1. 1990 Electric Society All Japan Meeting Lecture Thesis Collection No. 874 "Study of Toroidal Superconducting Magnetic Energy Storage (SMES) System."

Toroidal SMES Principle-Demonstration System

916C0018 Tokyo TEION KOGAKU CHODENDO GAKKAI YOKOSHU in Japanese 23-25 Nov 90 p 220

[Article by Takashi Sasaki and Katsuyoshi Toyoda, Mitsubishi Electric Corporation; Seiichiro Terai and Daiji Mizuguchi, Kansai Electric Power Co., Inc.; and Yoshishige Murakami, Engineering Department, Osaka University]

[Text] **1. Introduction**

Superconducting coils for superconducting magnetic energy storage (SMES) must be stable against input/output like alternating current (ac loss). Nb_3Sn coils have a high critical temperature, possess temperature margins, and are likely to be used as this type of coil for alternating current. However, they must be heat treated at high temperatures, and this makes it difficult to provide appropriate cooling channels within coils. Their features, therefore, have not to date been able to be utilized effectively. We resolved this problem by developing spacers, and confirmed specific features as described below. As a result, we have been able to ensure the prospect for the use of Nb_3Sn coils for SMES, and report on the outline.

2. Specifications of Wires and Coils

Table 1 presents the specifications of the superconducting coil and wire. Figure 1 shows the coil structure. Superconducting element wires of 0.8 mm each in diameter were insulated with T glass and wound in a stainless reel. A heat resistant spacer with good insulation and mechanical characteristics was provided between layers as a cooling channel. To improve the current density of the superconducting coil thus fabricated, a spacer was inserted at every three layers of the solenoid winds. The same spacer was used for insulation to ground. After formation, this Nb_3Sn coil was heat treated, impregnated with epoxy resin in vacuum, and cured, in order to increase its strength. Cooling channels were secured after impregnation with epoxy resin and curing.

3. Excitation Test

This coil was combined with a chopper panel for testing. Figure 2 shows the results of the tests.

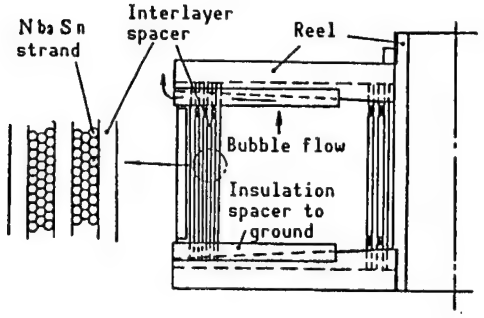

Figure 1. Coil Structure

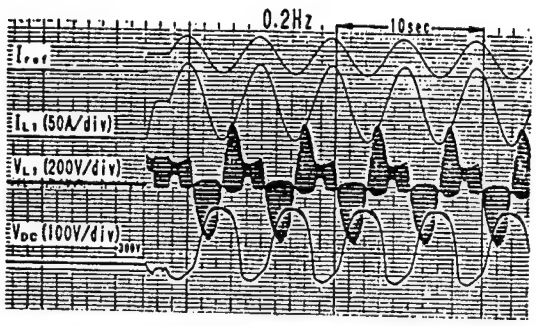

Figure 2. Sine Wave Excitation/ Demagnetization

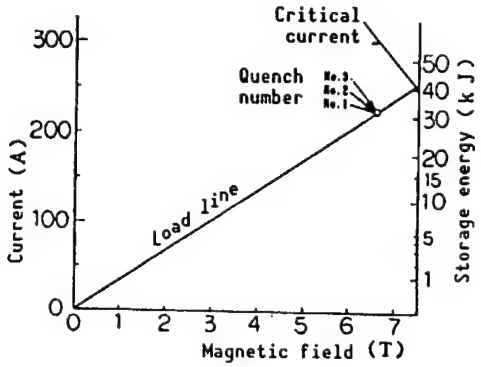

Figure 3. dc Excitation Quench Characteristics

Table 1. Specifications of Superconducting Coil

Maximum storage energy		32 kJ
Cooling system		Cooling immersed in liquid He, with a cooling channel impregnated with epoxy resin every three layers
Supercon-ducting wire	Element wire diameter	0.8 mm
	Cu ratio	2
	Element wire insulation	T glass
Size of coil portion (inner radius x outer radius x height)		35 x 130 x 74 mm
Cooling channel spacer		Stainless steel + braid over braid alumina fiber
Maximum current		227 A
Coil portion mean current density		114 A/mm^2
Maximum empirical magnetic field		6.6 T

The magnetic field generated at a sine wave peak current (I_{L1} = 170 A) was 5 T. Further, we repeatedly conducted tests on high-speed excitation/demagnetization (5 T/s, B_{max} = 5 T), and confirmed that Nb_3Sn coils can be used as SMES system coils for inputting and outputting like alternating current. Figure 3 shows the quench characteristics during dc electrification.

Toroidal SMES Principle-Demonstration System

916C0018 Tokyo TEION KOGAKU CHODENDO GAKKAI YOKOSHU in Japanese 23-25 Nov 90 p 221

[Article by Katsuyoshi Toyoda and Keiki Itami, Mitsubishi Electric Corporation; Seiichiro Terai and Daiji Mizuguchi, Kansai Electric Power Co., Inc.; and Yoshishige Murakami, Engineering Department, Osaka University]

[Text] **1. Introduction**

As a toroidal superconducting magnetic energy storage (SMES) system, a voltage type invertor plus chopper circuit system can be considered.[1] This system has many features such as easy group control of many superconducting coils and parallel/multiplex use of superconducting coils and converters. However, unlike excitation by the general dc stabilization power supply, chopped high voltage pulses are repeatedly applied in chopper excitation. This makes it difficult to detect the transition of superconducting coils to a nonsuperconducting state. The authors, et al., confirmed the possibility of detection of this phenomenon using boxcar integrators.

2. Method of Detecting Transition of Nonsuperconducting State During Chopper Excitation

Figure 1 shows a schematic of applied voltage and changes in current during chopper excitation. The figure shows that coil current increases in the form of a step, due to a repeatedly applied pulse voltage. A pulse voltage with a narrow width continues to be applied to compensate for the current attenuation due to circuit loss during the maximum current holding.

Figure 2 shows a block diagram of a nonsuperconducting transition detection circuit, and Figure 3 shows the principle of operation.

Using repeat signals as triggers, the boxcar integrator opens gates with a fixed width at a time that is delayed by a certain time from trigger signals, and takes only the signals corresponding to the fixed width. Thus, the boxcar integrator maintains outputs in proportion to inputs.

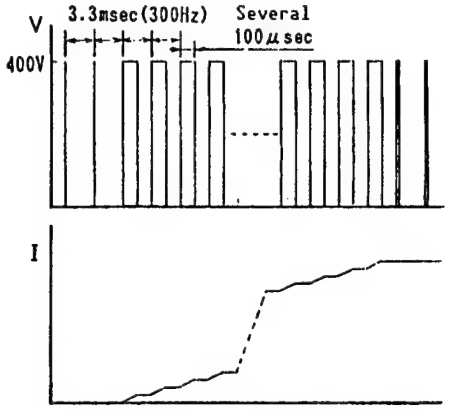

Figure 1. Schematic of Chopper Excitation

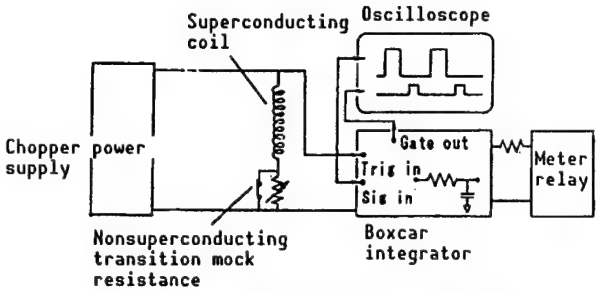

Figure 2. Nonsuperconducting Transition Detection Circuit

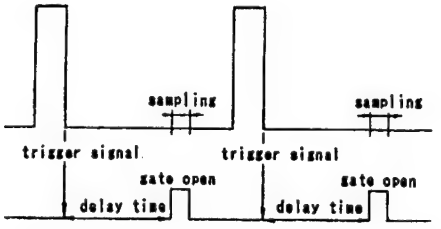

Figure 3. Principle of Operation

With a circuit as shown in Figure 2, it is possible for boxcar integrators to detect nonsuperconducting voltage produced in superconducting coils, without being affected by chopper voltage.

References

1. 1990 Electric Society All-Japan Meeting Lecture Thesis Collection No. 874 "Study of Toroidal Superconducting Magnetic Energy Storage (SMES) System."

100-kWh-Class Hybrid SMES

916C0018 Tokyo TEION KOGAKU CHODENDO GAKKAI YOKOSHU in Japanese 23-25 Nov 90 p 222

[Article by Yutaka Matsunobe and Kiyoshi Yamaguchi, Hitachi Laboratory, Hitachi, Ltd.; Yukio Ishigaki and Katsuhiko Asano, Hitachi Works, Hitachi, Ltd.; and Chikushi Hara and Kiyoshi Okaniwa, Technical Laboratory, Tokyo Electric Power Co., Inc.]

[Text] **1. Introduction**

With respect to a superconducting energy storage system, solenoid and toroidal systems are being studied. These systems, however, result in an extreme increase in the electromagnetic force of coils, requiring specific measures for support. The hybrid type superconducting magnetic energy storage (SMES) system offsets electromagnetic force by combining solenoid coils with toroidal coils, thereby ensuring the ease of support. We conducted conceptual design of a 100-kWh-class hybrid SMES system, and report on the results.

2. Features

The hybrid SMES was proposed as a rock bed-free system, having the following features:

(1) Solenoid coils and toroidal coils are combined with each other so that mutual electromagnetic force can be negated, thereby greatly reducing the electromagnetic support for SMES using rock beds.

(2) Energy is stored concurrently by solenoid coils and toroidal coils. This makes it possible to have a storage system that ensures a high energy density, compared with a system in which energy is stored individually by solenoid coils and toroidal coils.

3. Design and Study

Figure 1 shows a bird's-eye view of a 100-kWh-class hybrid SMES system, and Table 1 gives the specifications of the coils.

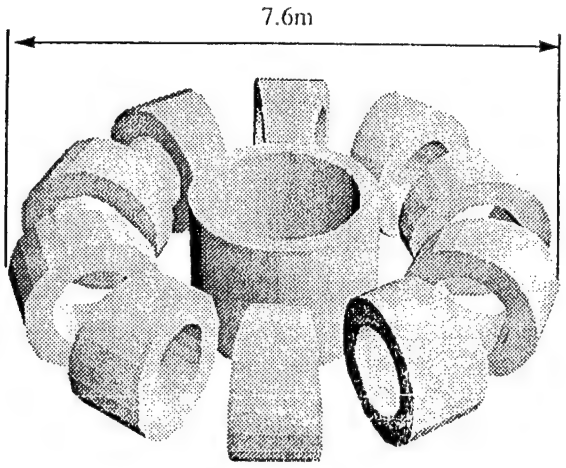

Figure 1. Hybrid SMES

Table 1. Specifications of Hybrid SMES Coils

Item	Unit	Solenoid	Toroidal
Large diameter	m		2.8
Small diameter	m		0.8
Coil total height	m	2.0	2.0
Outermost diameter	m	1.3	3.8
Innermost diameter	m	1.05	1.8
Rated current	A	50,000	50,000
Coil mean current density	A/m^2	2.0×10^7	2.0×10^7
Total compression force (centripetal force)	N	-1.3×10^8	1.3×10^8
Total number of winds	Turn	8 x 17	4 x 50
Storage energy	kWh	24.7	94.2
Energy ratio		0.2	0.8
Total energy	kWh	118.9	

We then obtained the specifications of solenoid coils and toroidal coils with the same storage capacity as that of hybrid coils, and compared their basic performance. The results are as described below.

(1) The area necessary to construct a hybrid coil is about 1.3 and 0.8 times, respectively, that for a solenoid coil and a toroidal coil.

(2) Electromagnetic force (hybrid coil: about 0 N):

- Solenoid coil: about 1.9×10^8 N
- Toroidal coil: about -1.4×10^8 N

These figures show that hybrid coils are superior to other types of coils. However, a new force known as "reversing force" operates.

(3) The area that requires the leak magnetic field of hybrid coils to be controlled to 0.01 T or smaller is about 0.3 times that of solenoid coils, and about 1.7 times that of toroidal coils.

References

1. "Research on Superconducting Energy Storage System [I]," Future Engineering Research Laboratory, May 1984.

Research on 2.5 MJ SMES Wires

916C0018 Tokyo TEION KOGAKU CHODENDO GAKKAI YOKOSHU in Japanese 23-25 Nov 90 p 223

[Article by Toshihide Nakano, Takayuki Irie, Kazuyoshi Hayakawa, and Makoto Fujiwara, Mitsubishi Heavy Industries, Ltd.; Daiji Mizuguchi and Seiichiro Terai, Kansai Electric Power Co., Inc.; Yoshishige Murakami, Osaka University,; and Takeshi Ogasawara and Yoji Kubota, Nihon University]

[Text] **1. Introduction**

Superconducting magnetic energy storage (SMES), aimed at stabilizing electric systems, are presumed to be subject to rapid changes in magnetic field. For efficiency and stability, it is therefore necessary to select wires with low ac loss for use in SMES. In this research, we evaluated the effect of ac loss given by filament diameters, twist pitches, and matrix ratios, based on experiments using several types of wires. Further, we conducted experiments on the stability and nonsuperconducting propagation characteristics using the same sample wires, and intend to report on the results in the next report.

2. Experiment and Results

Table 1 presents the specifications of the coil fabricated.

Table 1. Specifications of Coil

Item		Specification
Small coil	Inner diameter	330 mm
	Outer diameter	670 mm
	Width	167 mm
Toroidal radius		900 mm
Rated current		350 A
Current density		50 A/mm^2
Maximum magnetic field		5 T

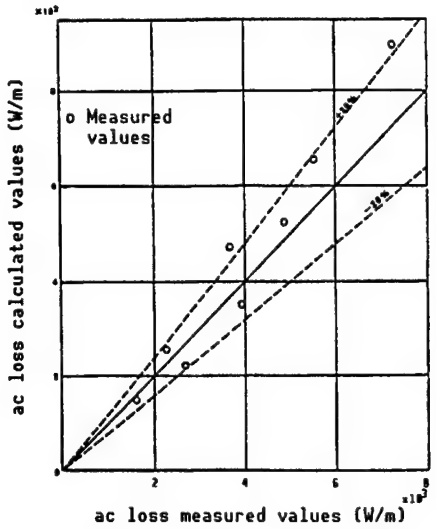

Figure 1. Results of Pulse Loss Measurement

This is a system in which six coils are arranged in the form of toroid. This system aims at confirming basic SMES functions and electricity system-stabilization functions and verifying technical problems; it is scheduled to be completed in 1993.

It is indispensable to attain low ac loss in wires by carrying out pulse (ac) operations as a system. As wires to be used in these coils, therefore, we used materials with specifications as given in Table 2, and measured their ac loss.

Table 2. Specifications of Specimen Wires

Type of wire	A	B	C	D
Wire diameter (mm)	0.701	0.701	0.311	0.785 x 0.397 (rectangular)
Filament diameter (μm)	3.89	3.89	1.53	6.0
Filament twist pitch (mm)	15.7	25.6	15.7	8.0
Matrix ratio (NbTi/Cu/CnNi)	1/0.37/2.9	1/0.37/2.9	1/0.37/2.9	1/1.31/0.42

Wires A through C consist of the same matrixes and use filament diameters and twist pitches as parameters. Wire D uses matrix ratios as parameters. In this experiment, we measured ac loss in wires using two types of measuring methods: electric measuring method and thermal measuring method. With respect to magnetic field variation ratios, we conducted tests on 10 T/S, which is in the top level for pulse coil specifications.

As a result of the above tests, the following have been shown:

(1) Filament diameters are not proportional to hysteresis loss at several μm levels. Therefore, the reduction of filament diameters to attain low ac loss is not very effective.

(2) The use of a Kim–Anderson model makes it possible to estimate ac loss within a range of errors of about ±20 percent.

On the basis of the above test results and the stability and nonsuperconducting propagation characteristics test results (to be described in the next report), we selected the specifications for wires used for actual coils.

Research on 2.5 MJ SMES Wires

916C0018 Tokyo TEION KOGAKU CHODENDO GAKKAI YOKOSHU in Japanese 23-25 Nov 90 p 224

[Article by Takayuki Irie, Toshihide Nakano, Kazuyoshi Hayakawa, and Makoto Fujiwara, Mitsubishi Heavy Industries, Ltd.; Daiji Mizuguchi and Seiichiro Terai, Kansai Electric Power Co., Inc.; Yoshishige Murakami, Osaka University; and Takeshi Ogasawara and Youji Kubota, Nihon University]

[Text] **1. Introduction**

As research on 2.5 MJ superconducting magnetic energy storage (SMES) wires, we conducted tests on ac loss characteristics using low ac loss wires, and reported on the results in the last report. This time, we carried out research on stability and nonsuperconducting propagation characteristics that are important in determining wire specifications, and grasped the effects of characteristics of various types of wires based on experiments.

2. Experiment and Results

We used specimen wires with the same specifications (Table 1) as those of specimen wires described in the last report. Figure 1 shows the test system.

Table 1. Specifications of Specimen Wires

Type of wire	A	B	C	D
Wire diameter (mm)	0.701	0.701	0.311	0.785 x 0.397 (rectangular)
Filament diameter (μm)	3.89	3.89	1.53	6.0
Filament twist pitch (mm)	15.7	25.6	15.7	8.0
Matrix ratio (NbTi/Cu/CnNi)	1/0.37/2.9	1/0.37/2.9	1/0.37/2.9	1/1.31/0.42

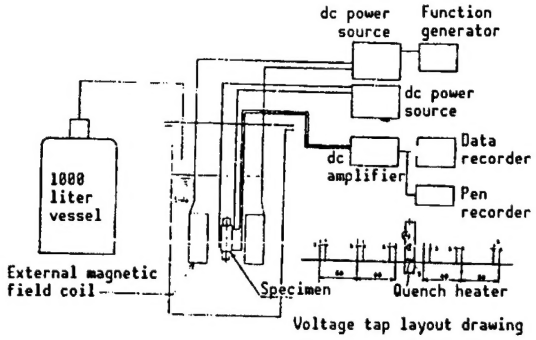

Figure 1. Test System

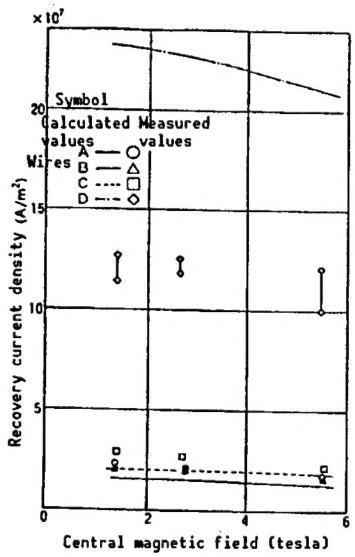

Figure 2. Results of Recovery Current Measurement

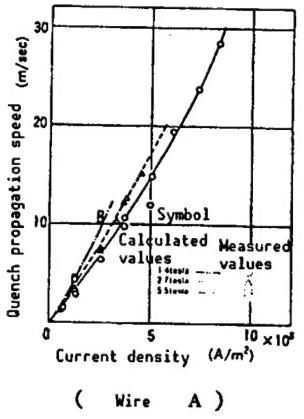

Figure 3. Example of Quench Propagation Speed Measurement

As shown in Figure 1, quenching was forcibly produced by directly heating wires with a heater, and the critical amount of heat and recovery current caused by quenching were measured.

The propagation velocity was calculated based on the time delay of the rise in voltage of each voltage tap.

The results of tests revealed the following:

(1) Recovery current can be relatively calculated based on the Maddock stabilization standard.

(2) The nonsuperconducting propagation can be evaluated using the Wilson equation.

On the basis of the above test results and the ac loss evaluation test results described in the last report, we selected actual coil wire specifications.

3. Future Plan

We intend to design and manufacture coils between fiscal years 1990 and 1991, and to conduct coil performance confirmation tests.

- END -